Theoretical and Applied Climatology (2025) 156:79
https://doi.org/10.1007/s00704-024-05264-3

RESEARCH

Spatiotemporal analysis of urban expansion, land use dynamics, and thermal characteristics in a rapidly growing megacity using remote sensing and machine learning techniques

M. Shahriar Sonet[1] · Md. Yeasir Hasan[2] · Abdulla Al Kafy[3] · Nobonita Shobnom[4]

Received: 4 August 2024 / Accepted: 30 October 2024 / Published online: 10 January 2025

Abstract

Global climate change and rapid urbanization are transforming land use and thermal environments, particularly in developing megacities, impacting regional climate and sustainable development. In cities like Dhaka, Bangladesh, urbanization has significantly altered land use and land cover (LULC), directly affecting urban climate and land surface temperature (LST).This study investigates the impacts of rapid urbanization on LULC changes and LST in Dhaka, Bangladesh, using multi-temporal satellite imagery from Landsat 5, 7, and 8 from 2009 to 2023. The classification analysis was conducted using Support Vector Machine classification and Random Forest (RF) modeling in Google Earth Engine to predict future LST. The classification achieved high accuracy, with kappa values over 80%. Results found that, due to the Dhaka Metropolitan Development Plan (DMDP) urban settlements expanded by 139.52 km², and vegetation and water bodies declined by 16.71% and 51.71% respectively. The study also found a 4 °C increase in LST (from 34 °C in 2009 to 38 °C in 2023), with predictions indicating further increases up to 41 °C by 2030. Statistical analysis revealed strong correlations between LST and LULC indices, with R^2 values of 0.42 and − 0.68 for NDVI and NDWI (negative correlations), and 0.04 and 0.26 for NDBI (positive correlation). The RF model, with an R^2 of 0.953 between observed and predicted values, further predicts a 3 °C rise in LST over the next decade. Spatial analysis revealed the highest urban expansion occurred in the northeastern and southeastern regions of the city. This study demonstrates the utility of integrating multi-temporal satellite data, machine learning, and spatial modeling to quantify urban growth patterns, associated land cover changes, and thermal impacts. The findings highlight the need for climate-adaptive urban planning in rapidly developing megacities to mitigate rising urban temperatures and associated environmental and health risks. The modeling approach presented can support evidence-based policymaking for sustainable urban development and climate change adaptation in Dhaka and similar urban contexts globally.

✉ M. Shahriar Sonet
sonet.m34@gmail.com

✉ Md. Yeasir Hasan
yeasirhasan28@gmail.com

Abdulla Al Kafy
abdulla-al.kafy@localpathways.org

[1] Geospatial Information Sciences, University of Texas at Dallas, 800 W Campbell Rd, Richardson, TX 75080, USA

[2] Department of Geosciences, Texas Tech University, Science Building, 1200, 125 Memorial Circle, Lubbock, TX 79409, USA

[3] Department of Urban & Regional Planning, Rajshahi University of Engineering and Technology, Rajshahi 6403, Bangladesh

[4] Research Consultant, Remote Sensing Division, Center for Environmental and Geographic Information Services (CEGIS), Dhaka 1207, Bangladesh

1 Introduction

Global scientific advancements are accelerating urbanization, impacting over 54% of the global population and surrounding areas, leading to economic growth (A.-A. Kafy, M. N. H. Naim, et al., 2021; Ullah et al. 2019). Urbanization, although promoting economic growth, has detrimental effects on cities in both the immediate and long-term (Abdullah et al. 2019; Faruque et al. 2022; A.-A. Kafy, M. N. H. Naim, et al., 2021; Rahman et al. 2020). Land use shifts highlight the impact of urbanization on ecological sustainability, transforming natural landscapes into developed areas, and affecting vegetation and water resources by reducing them (A.-A. Kafy, M. Islam, Kafy et al. 2021a, b, c, d, e; Li et al. 2017a, b; Tadese et al. 2020; Ullah et al. 2019;

Xu et al. 2020; Yirsaw et al. 2017). Human colonies have inhabited 1–6% of the surface of the universe, and during the last three centuries since 1900, there has been a global decline of 19% in forests and 8% in grasslands (Ahmed et al. 2019, 2021; Rahman et al. 2020; Reis 2008; Tadese et al. 2020; Ullah et al. 2019). Urbanization and land use changes influence ecosystems and water supplies as people and economies grow, but they raise LSTs by 2–4 °C. Population increase and economic advancement cause urbanization and land use changes, which harm ecosystems and raise LSTs. (Dey et al. 2021; Han et al. 2015; Hossain and Rahman 2022). Unregulated rapid urban expansion and alterations in land use and land cover land use and land cover (LULC) may alter the hydrological, thermodynamic, and radiation mechanisms of the surface of the planet, hence intensifying the effects of climate change and high temperatures (Ahmed 2011; Ahmed et al. 2019; Byomkesh et al. 2012). Furthermore, the unregulated modification of LULC increases urban areas by replacing vegetation, leading to environmental deterioration via urban heat island (UHI) effects (Dey et al. 2021; A. Kafy et al. 2021a, b, c, d, e). Built-up areas have a heightened UHI effect due to an increase in impervious surfaces. Sustainable management must tackle urban heat islands due to their many adverse consequences on city inhabitants (A.-A. Kafy, A. Al Rakib, K. S. Akter, et al., 2021; Kafy et al. 2020). Specifically, historic medium-resolution Landsat imagery delineates the land surface temperature (LST) and describes the UHI impact (A.-A. Kafy, M. Islam, Kafy et al. 2021a, b, c, d, e; Naserikia et al. 2019). Rapid urbanization increases impermeable surfaces, such as buildings, roads, and industries, leading to a significant rise in LST (A.-A. Kafy, A. Al Rakib, K. S. Akter, et al., 2021).

The spontaneous growth of urban regions in developing nations such as Bangladesh has a substantial effect on changes in LULC (Dewan et al. 2012; M. A. A. Hoque et al. 2016; Hossain and Rahman 2022). Many authors (Hoque et al. 2016; M. A. A. Hoque et al. 2016a, b; Islam et al. 2020; A.-A. Kafy, A. Al Rakib, K. S. Akter, et al., 2021; Kafy et al. 2020) use the "land use and land cover" (LULC) category to observe and evaluate the condition of ecosystems in metropolitan regions, natural habitats, and biological systems across many spatial scales. The evaluation of LULC, which encompasses both land use and land cover, is conducted jointly since these two factors are inseparable (Hassan and Southworth 2017; Hossain and Rahman 2022; Olofsson et al. 2014; Ullah et al. 2019). Researchers (Faruque et al. 2022; Hassan and Southworth 2017; Reis 2008; Yin et al. 2010) from a wide range of institutions have investigated the link involving LULC and LST dynamics in a variety of metropolitan areas. LULC shift analysis evaluates changes over time, assessing LST, urbanization, external influences, and ecological conditions, potentially reducing negative impacts on society and nature (Khan et al. 2015; Xu et al. 2020; Zhang et al. 2013). In emerging nations, fast use of natural resources owing to financial, socio-economic, and most of the cases, this infrastructural growth damages ecological sustainability (Islam et al. 2015; Li, Cao, Long, Liu, Li et al. 2017a, b).

The use of Remote Sensing (RS) and Geographic Information System (GIS) technologies has seen significant growth in assessing the changes in LULC and LST in metropolitan settings (Hassan and Southworth 2017; Islam et al. 2015; Wang and Xu 2010). GIS and RS applications are highly regarded for their ability to analyses ecosystem change, ecosystems, and global changes in climate (Hassan and Southworth 2017; A. Kafy et al. 2021a, b, c, d, e; Xu et al. 2020; Yirsaw et al. 2017). Along with these, Random forest (RF) (Dey et al. 2021) and Support vector machine (SVM) (Aldino et al. 2021) are known for their capabilities in processing multi-spectral images, including noise resistance, regression or classification, and unbalanced data set management. ImageRF (Simon et al. 2024) and ImageSVM (Rabe et al. 2010) are user-friendly applications designed to address the limits of LULC classifying with multi-spectral images. Thus, RF and SVM algorithms have been implied to improve the accuracy and efficiency of the classification process (A.-A. Kafy, M. Islam, et al., 2021; A. Kafy et al. 2021a, b, c, d, e; Naserikia et al. 2019). Multiple studies (Mallick et al. 2017; Mansaray et al. 2021; Naserikia et al. 2019) have been carried out in Bangladesh to analyze LULC utilizing a combination of Landsat multi-temporal imagery and integrating RS and GIS approaches. Detecting changes in LULC situations and monitoring LSTs by hands-on field visits is a laborious, prone to mistakes, and expensive process (Dey et al. 2021; Han et al. 2015; Tadese et al. 2020). RS and GIS technologies are used to assess, monitor, and simulate transformations in LULC as well as increases in LST (Ahmed 2011; A. Kafy et al. 2021a, b, c, d, e; Ullah et al. 2019). These technologies use spatiotemporal modelling techniques using data obtained from remote sensing (A.-A. Kafy, M. Islam, et al., 2021). The satellite imagery was analyzed using specific band arrangements to determine spectral indices, including the Normalized Difference Vegetation Index (NDVI), Normalized Difference Water Index (NDWI), and Normalized Difference Built-up Index (NDBI). NDVI represents vegetation cover (A. Kafy et al. 2021a, b, c, d, e), NDWI represents water bodies (Xu 2006), and NDBI represents impervious build-ups (Background; Naserikia et al. 2019). These indices are then used to illustrate the correlation between various land characteristics and LST. (A. Kafy et al. 2020, 2021a, b, c, d, e; Roy and Bari 2022; Xu 2006) useed the RF and regression analysis model for the prediction future LST estimation by using Google Earth Engine (GEE).

(A.-A. Kafy et al. 2021) indicated that the estimation and prediction of LULC shifting as well as seasonal surface temperature for the regions of Chattogram, and Cumilla. But there is no indication of area direction changes of that city where Dhaka has considered massive rate in urban growth (Hossain and Rahman 2022; Khan 2014). (Sonet et al. 2024; Faruque et al. 2022) noted that, RS and GIS methods are used to monitor changes by LULC in mangrove and coastal areas of Bangladesh. However, there is a correlation between LULC and LST, since global temperatures are increasing steadily. In previous studies researchers (Ahmed et al. 2021; M. T. Ahmed, Hasan, Ahmed et al. 2020a, b, c; M. T. Ahmed, Islam, Ahmed et al. 2020a, b, c, 2022) were not concerned with the urban growth impact caused by LST, rather only showed groundwater assessment and salt intrusion in coastal parts of Bangladesh. It has been suggested by (Kafy et al. 2020) that the multi-layer perception system Markov chain model may be used to analyses changes in LULC characteristics in Rajshahi City, Bangladesh. Urban heat brought on by rising temperatures and the effects of global warming are two issues facing the urban environment (Dey et al. 2021; Ismail and Jusoff 2008). Even rapid urbanization is occurring in Dhaka Metropolitan Development Plan (DMDP) zones, where man-made surfaces use more heat and have higher temperatures than vegetation-dominated regions (A.-A. Kafy, M. N. H. Naim, et al., 2021; Khan 2014). In DMDP regions, man-made surfaces have grown steadily in recent decades, and this has substantially increased urban growth and LST rates (Kafy et al. 2020). Moreover, tropical cyclone on Bangladesh's coastline have been drawing cold front from South to North and impacting the continuous landform in the coast also impacting the land use and overall economy of the region causing rapid movement of people to the city and helping in urbanization development works which has also been analyzed using GIS and RS (Sonet et al. 2024). However, it is important to note that the urban growth and LST rates are much greater in the conterminous DMDP area.

Recent research has been limited in examining the impact of changing LULC scenarios on LST in these large urban growth areas. This research focused on the DMDP area in Bangladesh, by using from Landsat 5, 7, and 8 satellite images to analyze changes in LULC and LST from 2009 to 2023. The objective is to examine the effects of urbanization on LST and LULC, changes in LULC over time, and the accuracy of these changes. The study also aims to analyze the correlation between LULC indices (NDVI, NDBI, and NDWI) and LST. The goal is to create a model that predicts future LST (2030) based on changes in LULC and LST scenarios from the previous year to 2023.

2 Study area

DMDP is situated on the Buriganga River, is the city region in Bangladesh with the highest population density, situated between the longitudes of 90°01′ and 90°37′ east and latitudes of 23°53′ and 24°06′ north (A.-A. Kafy et al. 2021) (Fig. 1a-d). This study area is situated in central, the capital of Bangladesh, is the most populous city in the nation and functions as its social, political, and financial center (Fig. 1.a). Surface elevation in the town ranges from 1 to 14 m, while the normal slope of built-up areas is between 6 and 8 m. The Buriganga river, the Turag river, the Tongi Khal river, and the Balu river are the four important river systems that surround it on all sides: the south, the west, the north, and the east, respectively (Islam et al. 2015; Tadese et al. 2020) (Fig. 1.b & c). Groundwater is the source of nourishment for alluvial waterways, that are waterways that start from the floodplain (A.-A. Kafy, A. Al Rakib, K. S. Akter, et al., 2021). The region is level and is located on a sandstone terrace that dates back to the Pleistocene epoch and is commonly referred to as the Modhupur terraces.

Centre of Bangladesh is the location of the study area, which incorporates two city corporations corporation within its boundary (Fig. 1). The region is situated between the tropical and subtropical rainfall regions and is characterized by climate conditions that are generally moist (Abdullah et al. 2019; A.-A. Kafy et al. 2021). The normal temperature in the town ranges from 11.5 °C to34.5 °C, and it gets a total of 2000 millimeters of rainfall annually, with more than 80% of the precipitation happening throughout the monsoon period (June to September) (BMD 2013; A.-A. Kafy, M. N. H. Naim, et al., 2021). The growth of the population of a city had a considerable influence on the city's roadways, industrial layout, open-air ecological, accommodation, and business sectors, as well as the city's economic and social circumstances (A.-A. Kafy et al. 2021; A.-A. Kafy, M. Islam, Kafy et al. 2021a, b, c, d, e; Khan 2014). The estimated population of the DMDP is over 12 million, a 41.5% increase from 2001. The population ratio in the region is 8229 people sq/km^2, above the national average of 976 inhabitants per km² (BBS 1998; A.-A. Kafy, M. N. H. Naim, et al., 2021). The process of urbanization in DMDP is fraught with both difficulties and opportunities (Fig. 1d) (Hossain and Rahman 2022). It contributes significantly to the national economy's 19% share of Gross Domestic Product (GDP), and it also plays an important role in social development and cultural improvement (BBS 1998). According to (Climate 2020; Hossain and Rahman 2022), (Fig. 2a) illustrates the average monthly total precipitation or rainfall days, moisture, number of wet days, and typical amount of time of sunlight in Dhaka district and DMDP areas.

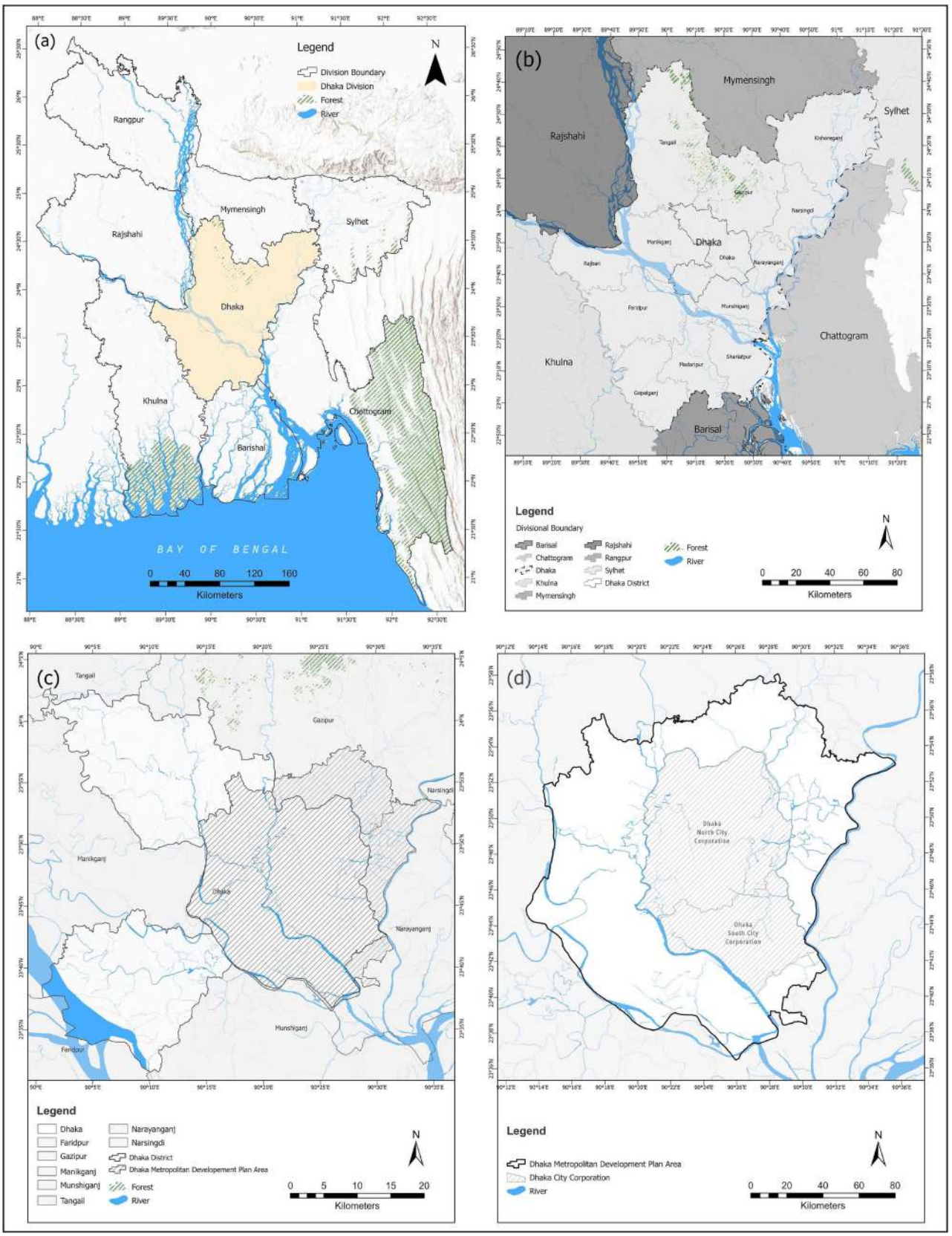

Fig. 1 The identification map of this research region (**a**) Bangladesh, (**b**) Division Boundary, (**c**) Dhaka Division and Dhaka District, and (**d**) DMDP Boundary

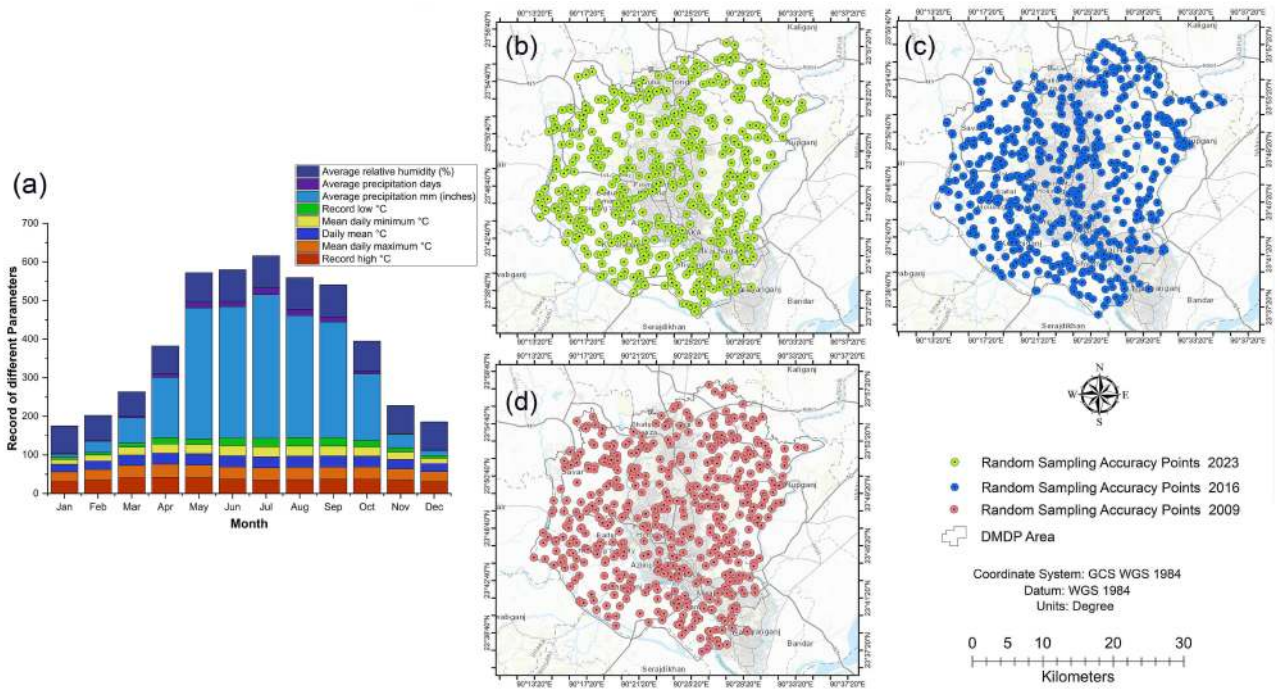

Fig. 2 The average monthly rainfall, moisture, and wet days condition (**a**), the random sampling areas used for the LULC class identification (**b-d**)

Table 1 The LULC classification system and its corresponding class summaries

LULC Class	Description
Water Body	Rivers, lakes, wetlands, and permanent open water body
Urban Area	Transportation, roadways, mixed urbanized residential, business, manufacturing, and other build-up area
Vegetation	The agricultural region encompasses several types of land, including cultivated land, fallow lands, vegetable property, deciduous forests, forest-covered lands, palm trees, trees scrub, and other vegetation types.
Bare Land	Uncovered soils, places of waste disposal, and regions of ongoing excavations

3 Materials and methods

3.1 Datasets

This research has used Landsat 5 TM Collection 2 Tier 1 TOA Reflectance, Landsat 7 Level 2, Collection 2, Tier 1, and Landsat 8 Collection 2 Tier 1 Raw Scenes satellite images with 10% cloud coverage. The raster images and acquisition dates are specified in Table S1. The United States Geological Survey (USGS) employs standardized data collection methods across several datasets over the years, so that it mitigates seasonal fluctuations, facilitating enhanced comprehension of longer-term patterns, identification of anomalies, and significant correlations among datasets (Byomkesh et al. 2012; Justice et al. 2002; A.-A. Kafy et al. 2021). Cloud free Landsat 5, 7 and 8 OLI/TIRS images were filtered and processed using ArcGIS Pro was used for GIS operations (LULC and accuracy analysis). Furthermore, the USGS website (https://earthexplorer.usgs.gov) makes Landsat data accessible without charge (Hassan and Southworth 2017; Islam et al. 2015; A.-A. Kafy et al. 2021; Mansaray et al. 2021; Reis 2008).

3.2 Preprocessing of datasets

This investigation used Landsat's satellite information to determine the spatial distribution of LULC classifications (A.-A. Kafy, A. Al Rakib, K. S. Akter, et al., 2021) (Table 1). Data preprocessing was carried out via the ArcGIS Pro tools. The Landsat 5, 7 and Landsat 8 datasets were resampled to a 30 m resolution and reprojected to the WGS 84/UTM zone 46 N coordinate system (Justice et al. 2002; Wang and Xu 2010). This study also used Landsat's surface reflectance bands (Table S1) to calculate terrestrial LST in GEE. The research also analyzed the three indices to create indices based on the spectral distribution of solar reflectance. The satellite photos were then examined with ArcGIS Pro. The study's entire procedure is represented in Fig. 3.

3.3 Evaluation of land use and land cover changing

The classification technique for images involves using multidimensional data to categorize LULC characteristics into distinct groups (Table 1) (Aldino et al. 2021; Rahman

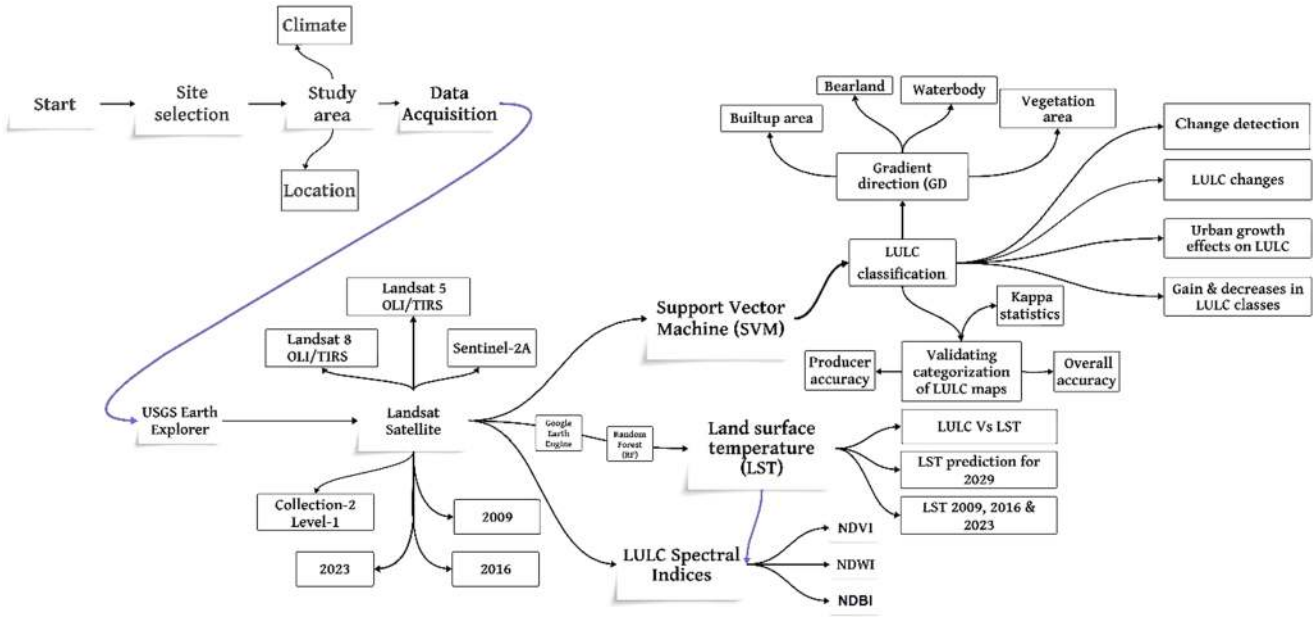

Fig. 3 Methodological Flowchart

et al. 2020). Scholars have presented numerous supervised and unsupervised categorization techniques (Aldino et al. 2021). The supervised classification strategy implemented the SVM classifier, which selects retraining units for picture categorization (Aldino et al. 2021; Ismail and Jusoff 2008). The scientists (Yin et al. 2010; Yirsaw et al. 2017; Zhang et al. 2013) used the SVM classifier to imagine the categorization, highlighting its superior accuracy compared to other approaches (Aldino et al. 2021; Liu et al. 2007). RF and SVM were evaluated to ascertain the optimal predictive approach based on performance metrics (Aldino et al. 2021; Sonet et al. 2024). Conventional statistical techniques have been used in most accident prediction in recent research (Aldino et al. 2021; A.-A. Kafy et al. 2021; Rahman et al. 2020; Roy et al. 2021). Time-series methodologies have been used for accident forecasting(Rahman et al. 2023; Ullah et al. 2019). The images in this study areas were categorized into four distinct groups: waterbody, urban area, vegetation, and bare land.(A.-A. Kafy, A. Al Rakib, K. S. Akter, et al., 2021; Siddiqua 2017) has indicated that 2015 has started the development of urbanization of DMDP areas. Besides some authors (Dewan et al. 2012; A.-A. Kafy, M. N. H. Naim, et al., 2021) stated that there is a significant effect of LST on the environment of overall Dhaka city. To determine the amount of change from water bodies, vegetation cover, bare land, and urban areas from 2009 to 2016, and from 2016 to 2023, the "combine" technique within the "spatial analyst toolset" in ArcGIS Pro software has been used. In ArcGIS Pro the combining tool was utilized to classify values in integers. It employs a confusion matrix to ensure a precise assessment of categorized images and identification data (Liu et al. 2007; Morshed et al. 2017; Wang and Xu 2010); Ward et al. (2011). The combine tool sequences several rasters in such a way that each individual combination of the input parameters has a distinct output value. The LULC sub-classes, with explanations, throughout the SVM classification process, are shown in Table 1.

3.4 Calculation of gradient direction (GD)

Geographic data evaluation is a process that enhances the resolution of small-scale data to summarize the spatial and temporal patterns of LULC (Cao et al. 2019; Faruque et al. 2022). Change in orientation estimation is a local investigation method that identifies unique land use and land cover patterns in different directions. This involves drawing dense spheres from the city center, expanding lines at five-kilometer intervals, and joining these lines to construct segment regions (Dewan et al. 2012; A.-A. Kafy, A. Al Rakib, K. S. Akter, et al., 2021). Each zone is distinguished by unique land use and cover classifications, identifying directional variances. The procedure included drawing concentric circles outward from the city center at regular intervals. The greatest contiguous ring should include the whole research region, considering all land use and land cover categories. Secondly, extending rays from the metropolitan center at 5 km intervals defined 16 orientations (Hossain and Rahman 2022; A.-A. Kafy et al. 2021; A.-A. Kafy, M. N. H. Naim, et al., 2021). The focused circles intersecting those lines formed section regions. Finally, distinct LULC categories were used for every single segment zone to identify

orientation variances (A.-A. Kafy et al. 2021; Kafy et al. 2020; Y. Li et al. 2017a, b).

3.5 Accuracy of LULC dataset

The accuracy evaluation included calculating the overall accuracy, user accuracy, producer accuracy and kappa statistics. This is considered one of the most effective quantitative methods for evaluating picture classification efficiency. It is assessed the correctness of the divided maps by overlaying 500 randomly selected ground truth images from Google Earth Pro (Avdan and Jovanovska 2016; Hassan and Southworth 2017; Hossain and Rahman 2022; A.-A. Kafy et al. 2021) (Fig. 2b-d) for each year. In this research, 500 GPS locations were randomly chosen for accuracy analysis in each year of land use and land cover LULC maps categorization, based on (Olofsson et al. 2014) shows on (Fig. 2b-d).

3.6 Calculating the process of LST

The single-channel (SC) approach was used to calculate the LST using Landsat thermal infrared readings. Both Landsat 5, 7 and Landsat 8 include thermal bands, while Landsat 8 stands out as the only satellite with two thermal bands (A.-A. Kafy et al. 2021; A.-A. Kafy, M. N. H. Naim, et al., 2021; Kafy et al. 2020). The Eqs. (1), (2), (3), (4), (5), (6), (7), and (8) were used in the GEE to compute the LSTs. Description of overall dataset used for LST has been shown on Table S1.

3.6.1 LST estimation for landsat 5 and 7 TM

The calculation of spectral radiance was performed using Eq. (1) (Cao et al. 2019; A.-A. Kafy, A. Al Rakib, K. S. Akter, et al., 2021; A.-A. Kafy et al. 2021).

$$L_y = \left(\frac{LMAX_y - LMIN_y}{QCALMAX - QCALMIN}\right) .(QCAL - QCALMIN) + LMIN_y \quad (1)$$

The spectral radiance, temperature (or LST) has been calculated by the use of Eq. (2). (Islam et al. 2015; A.-A. Kafy, A. Al Rakib, K. S. Akter, et al., 2021; Kafy et al. 2020)

$$T = \frac{K2}{ln\left(\frac{K1}{L_y} + 1\right)} - 273.15 \quad (2)$$

3.6.2 LST calculation for 8 OLI/TIRS

The major source of information for this research is the Landsat 8 archives provided by the USGS, which contain the GEE data catalogue. The conversion of digital number data (DN) to Top of Atmospheric radiance (TOA) was performed using Eq. (3).(Faruque et al. 2022; Y. Li et al. 2017a, b; Mansaray et al. 2021)

$$(TOA) = M_L \times Q_{Cal} + A_L \quad (3)$$

The brightness temperature was determined by using Top of Atmosphere (TOA) and two thermal transformation constants in Eq. 4 (Avdan and Jovanovska 2016; Dewan et al. 2012; A.-A. Kafy et al. 2021).

$$\text{Brightness Temperature (BT)} = \left(\frac{K_2}{\left(ln\left(\frac{k_1}{TOA}\right) + 1\right)}\right) - 273.15 \quad (4)$$

The NDVI has been used the Eqs. (5) and (6) to perform the calculation of the NDVI and the amount of vegetation (Avdan and Jovanovska 2016; Cao et al. 2019; Dey et al. 2021; Tadese et al. 2020).

$$NDVI = \frac{(Band\,5 - Band\,4)}{(Band\,5 + Band\,4)} \quad (5)$$

The surface's emissivity refers to its radiating capacity in relation to a black substance (Faruque et al. 2022; Mansaray et al. 2021; Roy et al. 2021).

$$Proportion\ of\ vegetation\ (P_v) = ((NDVI - NDVI_{min})/(NDVI_{max} - NDVI_{min}))^2 \quad (6)$$

The calculation is performed using Eq. (Cao et al. 2019; Kafy et al. 2020; Roy et al. 2021)

$$Emissivity\ (\epsilon) = 0.004 \times P_v + 0.986 \quad (7)$$

Equation 8(Roy et al. 2021) performs the calculation of LST.

$$LST = \left(\frac{BT}{1 + \left(0.00115 \times \frac{BT}{1.4388}\right) \times Ln\,(\epsilon)}\right) \quad (8)$$

3.6.3 *Prediction of LST*

The results of this study use the RF algorithm as the approach for predicting LST (Kafy et al. 2020, 2021a, b, c, d, e). This technique is specifically developed to calculate LST using data from the Landsat series of satellites. It is incorporated into GEE (Zhang et al. 2013). The technique was conducted in GEE (code available here).

Table 2 Evaluating the reliability of the categorized LULC using the confusion matrix method

Year/ Class Name	User Accuracy				Producer Accuracy				Overall Classification Accuracy	Kappa Statistics
	Water Body	Urban area	Bare land	Vegetation	Water Body	Urban area	Bare land	Vegetation		
2009	0.872	0.863	0.9	0.88	0.875	0.85	0.94	0.84375	0.881	*0.877*
2016	0.98	0.984	0.943	0.992	0.962	0.983	0.97	0.968	0.9812	*0.963*
2023	0.846	0.99	0.96	0.96	0.942	0.976	0.856	0.9847	0.944	*0.939*

Table 3 The spatial distribution of various LULC classifications in the research region between 2009 and 2023

Class Name/Year	Area (km^2)			Net Change (km^2)			Net Change (%)		Overall Change (%)
	2009	2016	2023	2009–2016	2016–2023	2009–2023	2009–2016	2016–2023	
Bare land	86.6827	124.085	81.6771	37.4023	-42.407	79.8093	43.1485	-48.922	92.0705
Urban area	220.554	258.736	370.117	38.182	111.381	149.563	17.3118	50.5005	67.8123
Vegetation	416.104	368.842	345.901	-47.262	-22.262	-69.524	-11.358	-5.3501	-16.7081
Waterbody	155.364	127.035	75.0179	-28.329	-52.0171	-80.3461	-18.233	-33.48	-51.713

3.7 Estimation of spectral indices

Spectral indexes, often referred to as land cover indicators, are essential in the determination of LST for many applications (Hossain and Rahman 2022; A.-A. Kafy, A. Al Rakib, K. S. Akter, et al., 2021; Khan 2014; Zhang et al. 2013). The indices, which include the NDVI (Y. Li et al. 2017a, b; Rouse et al. 1974), NDWI (Xu 2006), and NDBI, were calculated using Landsat Surface Reflection data from the years 2009, 2016, and 2023 (A.-A. Kafy et al. 2021; Rahman et al. 2020). Table S2 shows the scientific names of these the spectral indexes as well as their formulae and references to the relevant literature. NDVI and NDWI have significance for monitoring the state of vegetation, with NDWI being particularly important in controlling surface-water supplies and tracking situations of drought (Ahmed 2011; Kafy et al. 2020). Additionally, NDBI is a favored index for extracting information about built-up areas (Mansaray et al. 2021; Zhang et al. 2013).

4 Result and discussion

This section provides a concise overview of LULC changes using the SVM technique in three distinct years. The following discussion elucidates the conversion of various LULC categories, as well as the geographical distribution of changes in LULC classes utilizing GD analysis. The chosen research year included an assessment of LST as well as an evaluation of the link between LST and indicators like NDVI, NDWI, and NDBI. Additionally, the LST model was used to forecast future LST in the DMDP region using the random forest method.

4.1 Evaluation of LULC classes

In this study's SVM method has been used to ascertain the LULC change trends from 2009 to 2023. The assessment of classification accuracy involved measuring user accuracy, producer accuracy, kappa coefficient, and total accuracy. The images had an overall accuracy of 0.881, 0.9812, and 0.944, whereas the overall kappa values were 0.877, 0.963, and 0.939 for the years 2009, 2016, and 2023, as shown in Table 2. Producer accuracy for specific categories of LULC was highest for waterbody (0.96), urban areas (0.98), and bare land (0.97), all recorded in 2016, while only vegetation achieved an accuracy of 0.98 in 2023. Furthermore, the accuracy metric was calculated using the confusion matrix, which includes both the Producer's and the User's accuracy (Aldino et al. 2021; Dewan et al. 2012; Faruque et al. 2022). Again, according to the statistical analysis of Cohen's Kappa, the kappa coefficient value of 0.80–0.90 indicates a significant level of acceptance, with data dependability ranging from 0.64 to 0.81 (Dewan et al. 2012; Dey et al. 2021; Olofsson et al. 2014; Zhang et al. 2013). The kappa values in this investigation indicate a strong level of data reliability. During this time frame from 2009 to 2016, there was a consistent increase of 43.1485% in the amount of bare land, while there was a decrease of 48.922% as it was converted into urban areas, primarily, and other types of land by 2023 (Table 3). The rapid urban development had a substantial influence on both vegetation, with a net change of -11.358% and − 5.3501%, and waterbody areas, with a net change of -18.233% and − 33.48% during the years (2009–2016) and (2016–2023) shows on (Table 3; Fig. 4 (a-c), resulting in their conversion into growing cities. The growth of urban regions may be attributed to many variables, such as migration from the countryside to urban areas in pursuit of improved economic opportunities and the availability of

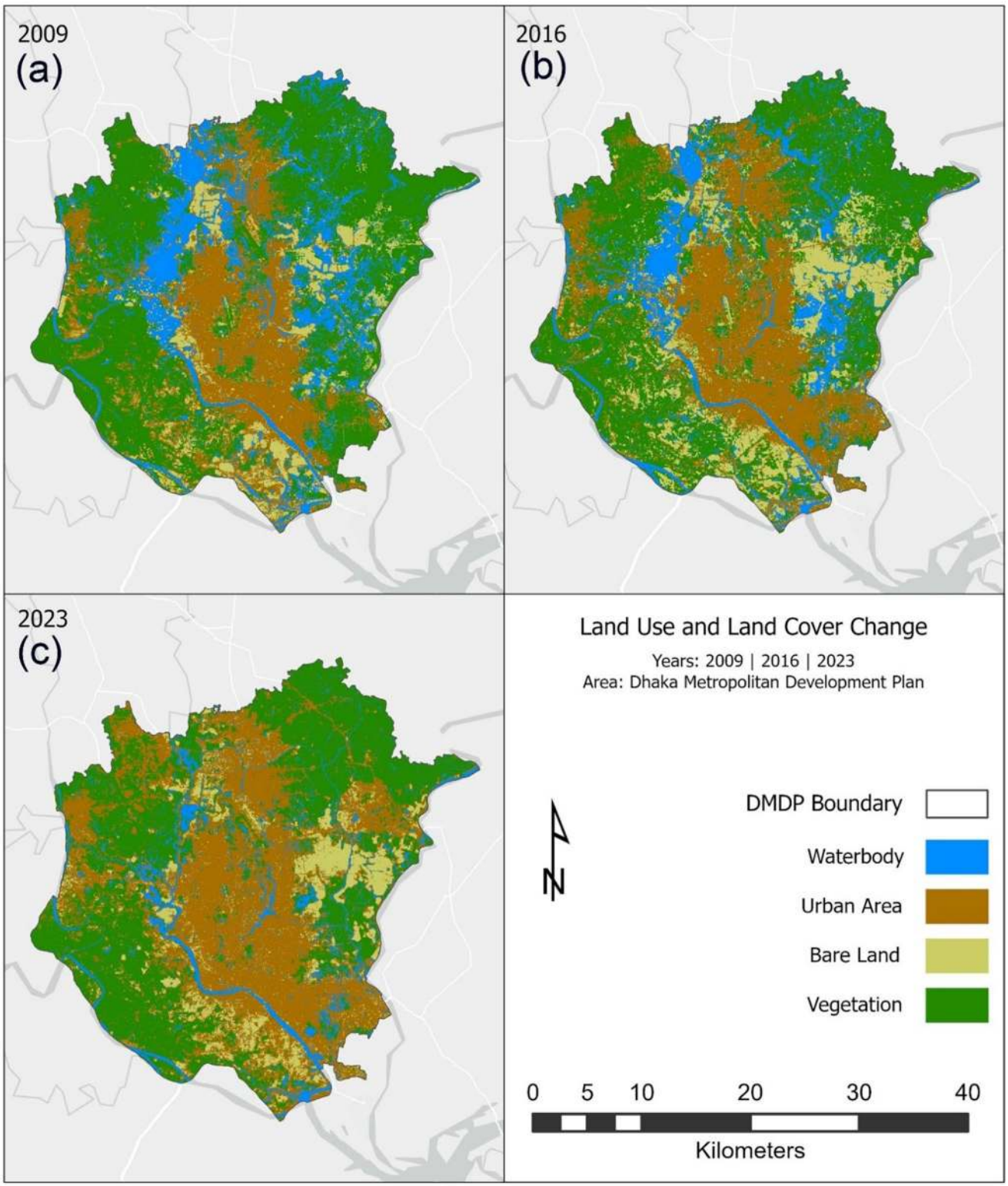

Fig. 4 LULC changes maps depicting changes in the research region between (2009–2023); Waterbody (blue); Urban area (dark brown); Bare Land (light brown); and Vegetation (dark green)

superior healthcare services in the examined region relative to the rural (A.-A. Kafy, A. Al Rakib, K. S. Akter, et al., 2021; Naserikia et al. 2019).

4.2 Transformation and decreases in LULC classes

The conversion rate among distinct LULC classifications is a crucial component in identifying the key factors that substantially contribute to shifts in LULC. The LULC growth in various LULC classes was determined by analyzing LULC transformation maps (Fig. 4a-c), as well as the gain and loss in different LULC classes (Fig. 5a-b). Additionally, the image comparison approach to estimate the LULC change, as presented in Table 3 and a corresponding Fig. 6(a-c). The LULC change maps show a decline in vegetation and waterbody area, while there is an increase in urban areas and barren land. In this context, specific land use categories have designated undeveloped land and open spaces as urban areas. The unaltered category demonstrates the consistency between distinct classes, such as urban areas remaining urban areas and bodies of water remaining unchanged during a three-year period (Fig. 5a).

According to the data provided in (Fig. 6a-c) and Table 3, it is evident that there were decreases in vegetation (-47.262 km^2 and − 22.262 km^2) and water bodies (-28.329 km^2 and − 52.0171 km^2) during the periods of 2009–2016 and 2016–2023, respectively. Conversely, urban areas showed growth (38.182 km^2 and 111.381 km^2), albeit with a negative correlation, while bare land increased by 37.4023 km^2 during 2009–2016 and decreased by 42.407 km^2 during 2016–2023, largely due to the DMDP project area. Throughout this timeframe, significant changes occurred across various land use and land cover LULC categories, particularly notable was the positive and substantial shift in urban areas. The rates of change observed for water bodies and vegetation areas were both strong and negative. Interestingly, urban areas remained unchanged during this period, which notably influenced the increased LST in the DMDP area.

4.3 Urban growth effects on LULC

The conversion rate among distinct LULC classifications is a fundamental element in identifying the key variables that are contributing substantially to changes in LULC. The research region is experiencing fast urban growth. To determine the effects of urban developments on other LULC categories, a combination tool was used to assess the impact (Fig. 5a-b).

From 2009 to 2023, massive changes have occurred in overall areas. Approximately 170 km^2 of vegetation area, 140 km^2 of barren region, and 98 km^2 of water bodies have been converted, and large areas have been transformed into urban areas (Fig. 5b).(Hossain and Rahman 2022) has also indicated that due to this kind of urbanization like DMDP area, the city landscape changed with LULC changes and affected the city's thermal environment. Even, fast urbanization has facilitated social and economic progress while simultaneously intensifying the depletion of scarce resources (A. Kafy et al. 2020, 2021a, b, c, d, e; Xu et al. 2020). However, it has also given rise to several environmental pollution issues, including water and air contamination and health concerns (Byomkesh et al. 2012; Rahman et al. 2020). Furthermore, the analysis revealed two significant and undesirable rates of change for the vegetation cover (-11.358% and − 5.3501%) and barren land (43.1485% and − 48.922%) Fig. 6(a-b). The forest area significantly declined over 14 years from 2009 to 2023, and rising surface temperatures have increased due to escalating deforestation. Consequently, the urban forest of DMDP lacks protection in contrast to the remote regions of the country, which have a significant annual destruction frequency (Yirsaw et al. 2017). Furthermore, in these findings, (Kafy et al. 2020) has recently documented a significant decline in the yearly coverage of vegetation in Dhaka city due to extensive development.(Siddiqua 2017) has suggested that there is a need for more vegetation areas in this city to enhance its safety. On the other hand, it has been observed positive changes in settlements (17.3118% and 50.5005%) from (2009 to 2016) and from (2010 to 2023) (Fig. 6a-c). The observed rise in the region's population in the early 2015s, after the formal designation of the study area as an economic zone inside the geopolitical zone, led to several alterations in the DMDP's LULC (Climate 2020; Hossain and Rahman 2022). The expanding population and economic expansion are leading to the increased use of spaces, waterbodies, and forest resources (Fig. 5a-b). The land cover modifications in the research region are mostly attributed to the local population, economic zone, and new colonial area. The tremendous economic growth of businesses in this region has significantly impacted local ecosystems, including water bodies, forest areas, and habitats.

Urban regions are undergoing rapid alterations in plant cover, bare land, and water bodies. Moreover, the results obtained from transforming the LULC map indicate that human actions lead to the conversion of forest areas into urban areas and water bodies (Fig. 5b) The proliferation of impervious surfaces primarily took place in the northeastern and southern sectors of the DMDP area (Fig. 5a). These changes in LULC result in variations in surface energy and affect the surrounding area's surface temperature conditions (Kafy et al. 2020; Naserikia et al. 2019). (A. Kafy et al. 2021a, b, c, d, e; Simon et al. 2024) has showed the effects of five socioeconomic factors, namely poverty, Gross Domestic Product (GDP), population density, distance to

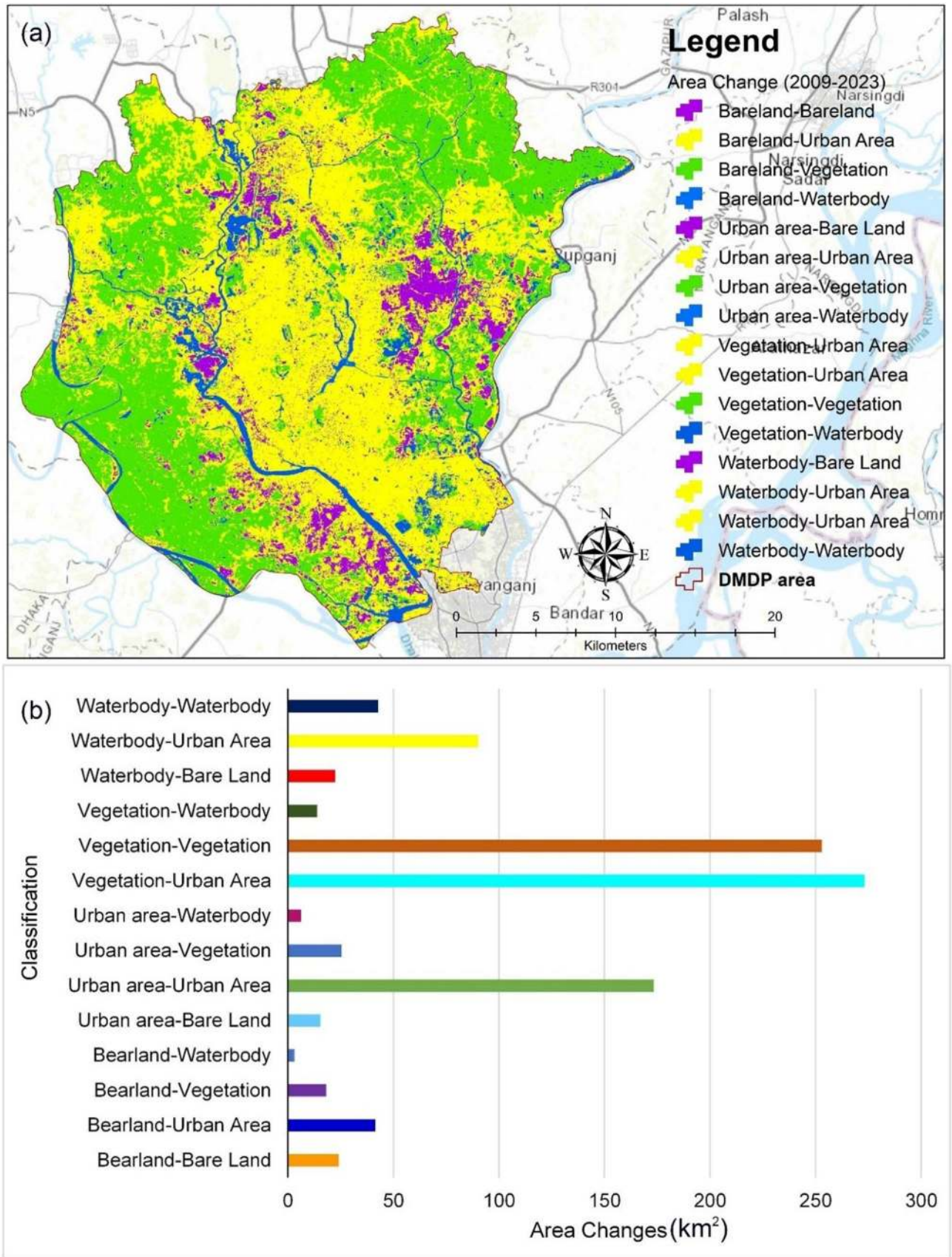

Fig. 5 Transformation of LULC classes losses and increase from (2009–2023); (**a**) Area changes where color is defined by changeable regions in right side - Waterbody (blue); Urban area (yellow); Bare Land (dark purple); and Vegetation (bright green), (**b**) Transformation of areas

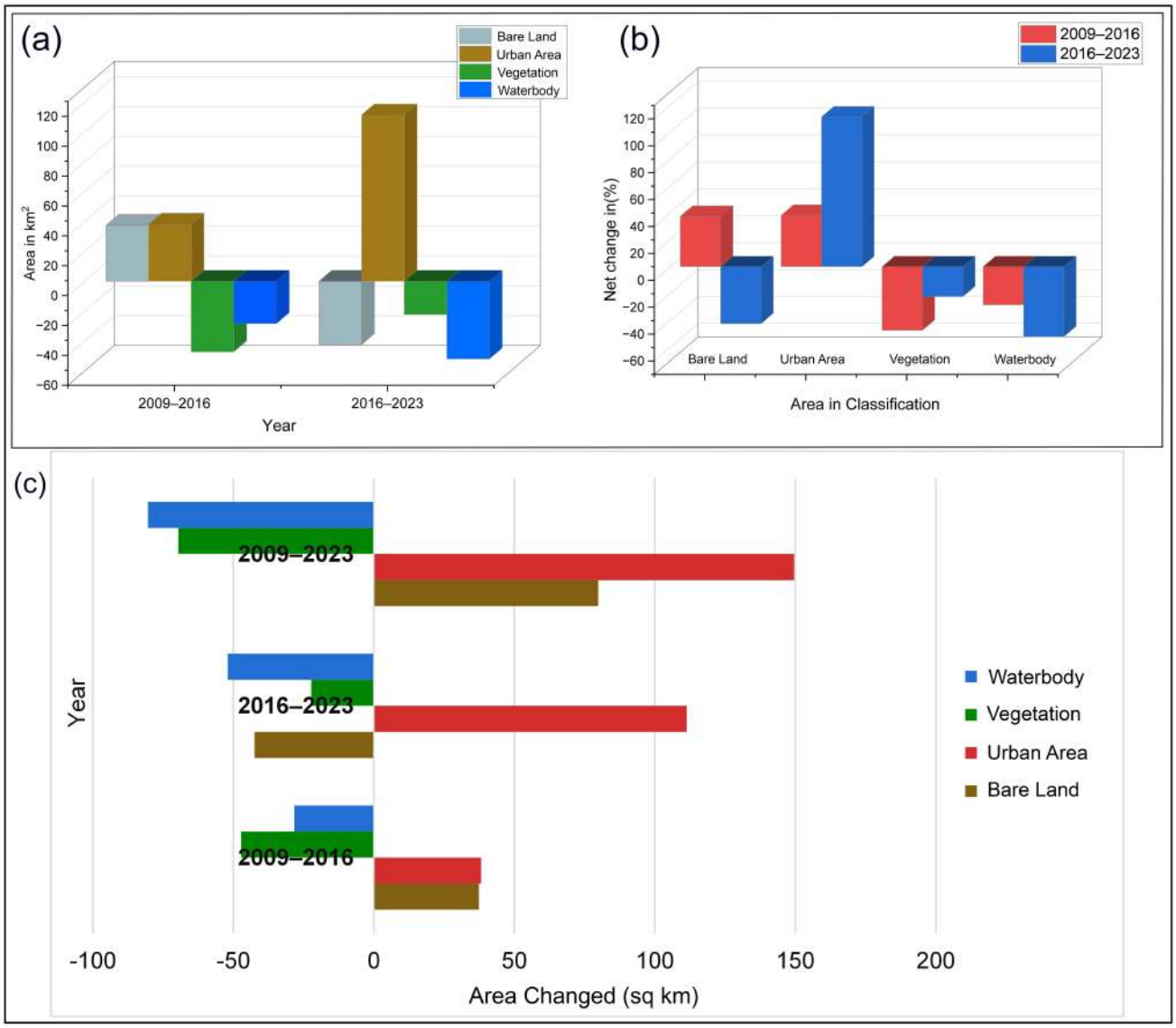

Fig. 6 Area basis LULC changes per year in (**a**) net changes (km^2) (**b**) percentage (%) & (**c**) total changes

the city center, and roads, have been assessed to understand their influence on LULC in the DMDP area. These variables represent economic growth, social spending, and transportation conditions. DMDP area is a pivotal economic center, making substantial contributions to several industries, such as commerce, banking, manufacturing, services, and tourism (Siddiqua 2017). The city accommodates crucial enterprises, governmental establishments, and global associations, while its harbor is a crucial entry point for exports and imports (Morshed et al. 2017). GDP has an indirect impact on changes in land cover, as well as an immediate effect on urban development and land use patterns. Economic development frequently results in heightened urbanization and infrastructural development, which in turn leads to alterations in land cover. According to (Fig. 5a-b), these kinds of changes occur as a result of infrastructure construction or the extension of bare land for additional development. This emphasizes the susceptibility of these places to environmental change that's increasing the LST (Dey et al. 2021; A. Kafy et al. 2020, 2021a, b, c, d, e).

4.4 Evaluation of the direction of change in LULC classifications

The Concentric circles are created from the city center to outside the research area border to determine the directional shifts of various LULC classifications. Directional analysis is a common technique used to summaries spatial-temporal urban growth and its effects on other LULC classifications (Figs. 7a-d and 8a-d).

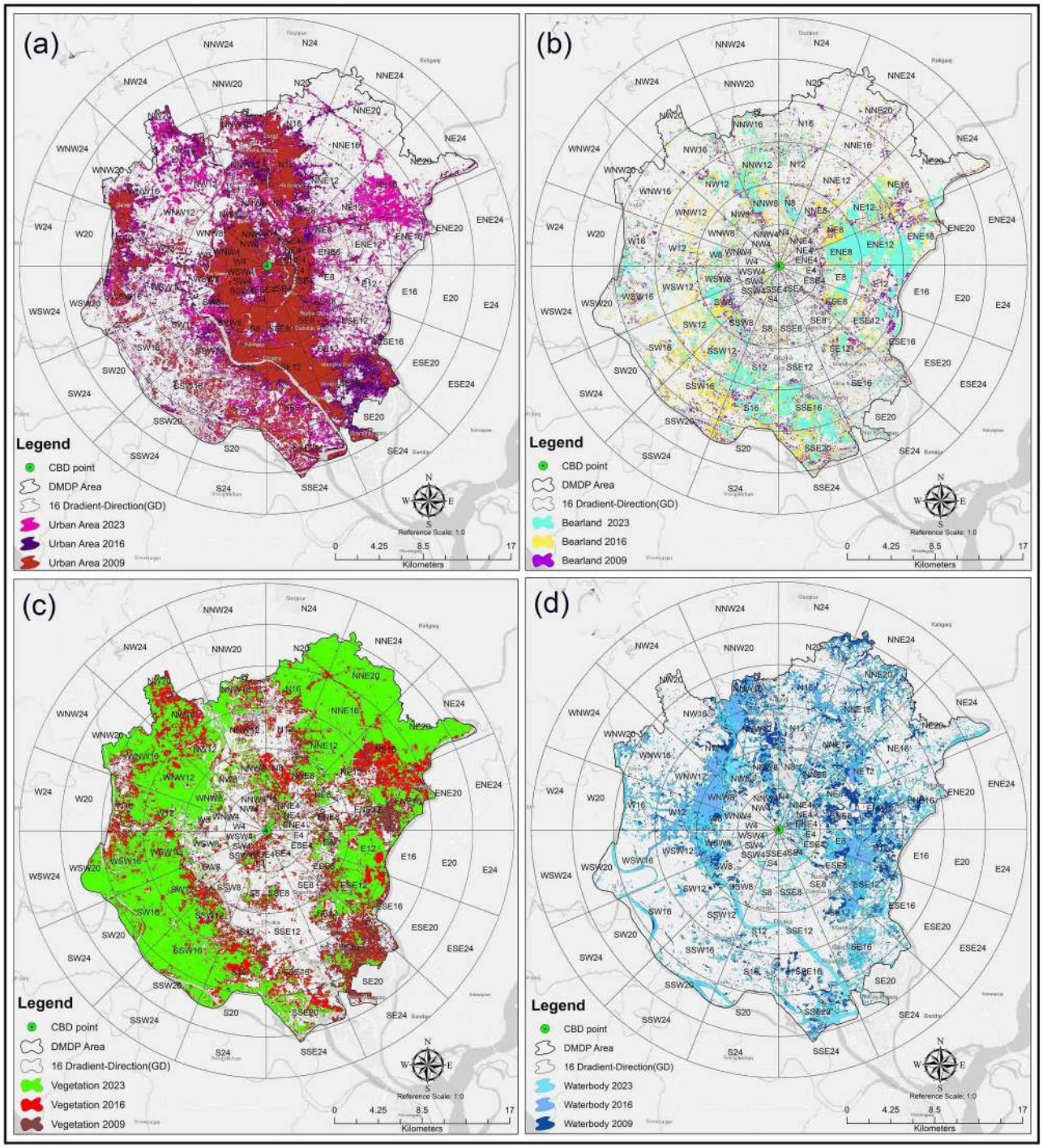

Fig. 7 (**a**) Urban area, (**b**) Bare land (**c**) Vegetation area and (**d**) Waterbody classes of LULC in 20 directional changes of the study area

4.4.1 Changes in urban area

Seven major cities around the globe had a significant metropolitan expenditure rate of more than 2.4% between 2009 and 2023 (Ahmed 2011; Dewan et al. 2012; A.-A. Kafy, M. N. H. Naim, et al., 2021). Dhaka is one of those seven cities(Tadese et al. 2020; Zhang et al. 2013). It is unfortunate that the growth has taken place and continues to take place at an alarming rate, especially considering the beginning of the 1990s (Morshed et al. 2017) and it has also increased at a higher rate in 2015 (Fig. 7a). This amazing rise in urbanization may be traced to five primary factors: migration from rural regions to urban areas, the creation of new employment possibilities, an improvement in its standard

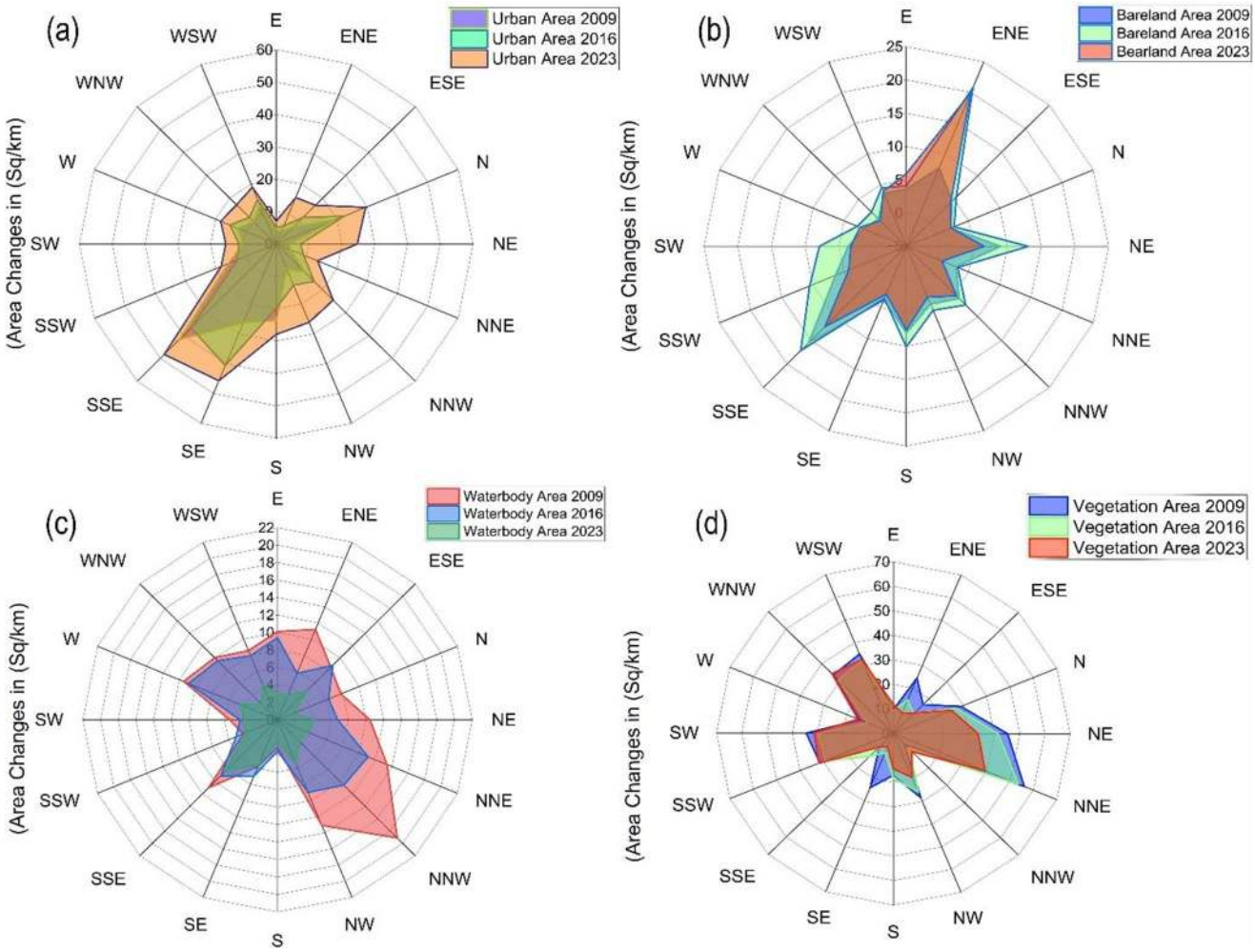

Fig. 8 Directional changes of investigation area (**a**) Urban area, (**b**) Bare land (**c**) Waterbody, and (**d**) Vegetation area

of living, growth by nature, and the redefining of metropolitan areas (Ahmed 2011; Hassan and Southworth 2017; Hossain and Rahman 2022). Based on the directional study according to (Figs. 7a and 8a.), it has been determined that fast urban growth has occurred in the northwest, northeast, and southeast areas. Even though urban growth is occurring considerably in every direction of the metropolitan area, the north (8.024%), north-to-east (6.71%), north-to-northeast (3.706%), north-to-northwest (6.66%), south-to-east, north-to-west (7.11%), south (7.590%), south-to-east (12.43%) and south-to-southeast (13.11%) directions are seeing significant urban growth due to the excellent management, business, entertainment, building, telecommuting, and transportation resources. Beijing is a case study for land-adaptive, spatial, and socio-economic aspects, where (Han et al. 2015) indicates that the LULC has changed due to urbanization, like DMDP areas. Urban growth is occurring at all levels of the municipality and these areas are more desirable to locals than any other area of the city because of all these amenities (Hossain and Rahman 2022; A.-A. Kafy et al. 2021; Kafy et al. 2020; Morshed et al. 2017). Demographic, economic, and cultural factors influence these extensive urban developments. Population growth and decline are significant determinants of LULC (Climate 2020; M. A. A. Hoque et al. 2016a, b). Furthermore, migration, the distribution of the rural-urban population, and industrialization influence it (BBS 1998).There are some socio-economic and policy factors, such as the expertise of land officers, together with political and economic policies and managerial competencies, that influence the ecological overall condition of DMDP (Dey et al. 2021; A. Kafy et al. 2020, 2021a, b, c, d, e). Additionally, the presence of these institutions is stimulating an increasing volume of institutional and business transactions, transforming the area into a hub of urban development. Marginalized rural inhabitants are compelled to migrate to these areas in pursuit of improved employment opportunities and an elevated quality of life (Morshed et al. 2017).

4.4.2 Changes in vegetation areas

Due to rapid urban expansion, the study area is considered one of the world's most undesirable towns in terms of quality of life due to rapid urban expansion. An ideal city should provide 25% of its total area for green spaces, as opposed to the only 5% designated under the DMDP (A.-A. Kafy, M. N. H. Naim, et al., 2021; Siddiqua 2017). According to the findings of the direction studies of transformation, there has been a decrease in the number of highly green areas in every direction of the metropolitan area. The city converted in that direction due to the presence of a greater non-urban to urbanized region, resulting in the most notable decrease of vegetation observed from (2009 to 2023) in east -to-north-east $(24.40\text{sq/km})_{2009} > (9.11\ \text{sq/km})_{2023}$, north-east $(45.24\ \text{sq/km})_{2009} > (33.56\ \text{sq/km})_{2023}$, north-west $(28.23\ \text{sq/km})_{2009} > (19.421\ \text{sq/km})_{2023}$, south-east $(23.95\ \text{sq/km})_{2009} > (5.862\ \text{sq/km})_{2023}$ whereas only small portion (north to northeast $(56.07\ \text{sq/km})_{2009} < (59.343\ \text{sq/km})_{2023}$ increased in the whole DMDP area (Figs. 7c and 8d). Urban designers and gardening professionals suggested that increasing tree planting and extending greenery in cities would support the urban forestry strategy in the Dhaka metropolis. Various initiatives are planting trees in different locations in DMDP (Byomkesh et al. 2012; Hassan and Southworth 2017; Khan 2014).(Faruque et al. 2022; Kafy et al. 2020; Siddiqua 2017) has been observed that although most of the cities in Bangladesh have seen tremendous expansion, the growth of vegetation in the general city area has not kept pace with their growth or the extremely high population rate.(Ullah et al. 2020) has also revealed that urban growth has makes a huge impact in Xi'an City, China as like as Dhaka city by reduction of vegetation which increased LST. Furthermore, (Kafy et al. 2020) shows the remote sensing techniques to examine the influence of LULC modifications on LST in the Rajshahi district of Bangladesh.

4.4.3 Changes in waterbody

Water bodies have played a crucial role in human society in several ways since prehistoric times. Water is the primary focus of the global tourism sector. Dhaka city has failed to effectively use its natural assets for water tourism expansion, despite having great potential similar to that of the Netherlands and Xi'an City, China (Dai et al. 2018; Ullah et al. 2020). Uncontrolled urban growth results from pollution and encroachment onto WBs instead of their conservation. Between (2016–2023), the volume of water bodies in the northwest increased due to water management improvements but significantly decreased in certain areas such as east (7.008km^2), east to north-east (8.168km^2), east to south-east ($3.882\ \text{km}^2$), north ($5.783\ \text{km}^2$), north-east ($6.343\ \text{km}^2$), north to north-east ($9.741\ \text{km}^2$), north-to-northwest ($15.64\ \text{km}^2$), and north-west ($7.774\ \text{km}^2$). The diminishing phenomena mostly occurred in a north-east direction (Figs. 7d and 8c). Several of the rivers, canals, and streams that formerly surrounded Dhaka have been partially filled in throughout the last 16 years, according to the city's history (Khan 2014; Morshed et al. 2017). The natural equilibrium was broken by the municipality's fast, uncontrolled urban expansion, which also made it the worst place to live every day (Morshed et al. 2017; Rahman et al. 2020).

4.4.4 Changes in bare land

Bare land is mostly undeveloped urban lands and open spaces that, because of the aesthetic and ecological features that they possess, provide many advantages to those who live in urban areas, including social, environmental, and economic advantages (A.-A. Kafy et al. 2021). During the categorization process, it was predicted that there was a growth in bare land, which was finally transformed into urban areas (construction of buildings, impermeable surfaces, highways, and so on). This was due to the enormous movement of people from rural areas to urban areas as well as a lack of focus on the preservation of open spaces (Figs. 7b and 8b). The assertion was supported by (Byomkesh et al. 2012; Dewan et al. 2012; Morshed et al. 2017) the increasing of urban area and development in the regions where bare lands have been rising because bare land has been considered as the pre-process of urban planning. Such as the east, east-to-northeast, east-to-south-east, north-east, north-to-northwest, and north-west, south-to-south-east, south-to-south-west, west-to-south-west directions have been increased alarmingly (Figs. 7b and 8b).

4.5 Relationship between LST vs LULC indexes (NDVI, NDWI, and NDBI)

4.5.1 Effects of changes with LST vs. indexes

The physical attributes of urban areas, including paved surfaces, road networks, and construction, are expected to be impacted by the features of LULC (Ahmed 2011; Byomkesh et al. 2012). Human activities and the growing global population's demand for natural resources drive these LULC features (Hossain and Rahman 2022; Morshed et al. 2017). This directly influences the formation of LST. Monitoring (LULC) changes is essential for identifying regional climatic patterns and quantifying unregulated or undesirable urban growth that is susceptible to ecological impacts (Zha et al. 2003). All the LULC indexes changes over the decade have been shown in Fig. S1. The average temperature in a city fluctuates at various locations, with the maximum

temperature occurring in urban centers and lower temperatures in outlying regions (Ullah et al. 2019). This highlights the significance of LULC in establishing land surface temperature LST data (Ullah et al. 2020). LULC data are essential for estimating the LST. There exists a mathematical correlation between LST and the above values, where NDBI values are directly proportional while NDVI and NDWI values are inversely proportional.

Vegetation areas demonstrate higher levels of NDVI in spatial analysis (Rahman et al. 2020). Consequently, there is an inverse relationship between the height of vegetation and the temperature (Cao et al. 2019; Kafy et al. 2020; Xu et al. 2020). Therefore, there is an inverse relationship between LST and NDVI, NDWI. The negative association between NDVI, NDWI, and LST is directly attributed to the elevated temperatures which is accepted by (Ullah et al. 2019; Xu et al. 2020). Another explanation (A.-A. Kafy, A. Al Rakib, K. S. Akter, et al., 2021; A.-A. Kafy et al. 2021; Karim and Mimura 2008) can be attributed to the fact that greenery, such as trees and vegetation, typically serve as absorbers and evaporator systems. They release water as steam, which leads to the retention of heat (A.-A. Kafy, A. Al Rakib, K. S. Akter, et al., 2021). The authors (A.-A. Kafy et al. 2021; Kafy et al. 2020; Khan et al. 2015) used numerous analyses to establish relationships during the investigation. The correlation between LULC indicators and LST is explained as follows. LST is influenced by air surface temperature, with urban and densely populated areas experiencing higher temperatures due to increased heat reflectivity (A.-A. Kafy, A. Al Rakib, K. S. Akter, et al., 2021; A. Kafy et al. 2021a, b, c, d, e).

4.5.2 Correlation of LST vs LULC indexes

All the correlation analyses revealed p-values below 0.05, indicating that the validation processes were statistically significant. The positive correlation between LST and NDBI, as well as the significant positive correlation between LST and NDWI, and the negative correlation between LST and NDVI are indicated in Fig. 9a-c. The examination of LST using NDVI, NDWI, and NDBI throughout all three study periods (2009, 2016, and 2023) has revealed a significant association, as indicated by the high R^2 values (Fig. 9a-c). In the realm of ecological analysis, a correlation is considered high when it approaches a value of 1. In the year 2023, the R^2 value was greater than in 2009 (Fig. 9a). Thus, a strong association is consistently detected across all time periods since the trendline accurately represents the data.

The east-northern part built-up areas were lower; on the other hand, the vegetation and water bodies were higher in 2009. But this ratio has been decreased to 2016 by converting bare land, which was increased by the DMDP project. During 2016–2023, the NDWI and NDVI decreased, while the buildup areas increased in those areas because of urban development, including rising population and industrial uprising (A.-A. Kafy et al. 2021; A.-A. Kafy, M. N. H. Naim, et al., 2021; Tadese et al. 2020). Based on (Fig. 9a-c), the relation of LST is associated with an inverse change in NDVI and NDWI. Conversely, the NDBI shows a positive rise. The LST temperatures in the east-south-central region are higher, whereas the southeastern region receives a higher LST due to construction projects and built-up areas. These places retain more heat because they are impervious and do not allow heat to escape as easily as the neighboring regions. Furthermore, this research discovered that both the NDWI and NDVI exhibit a decrease throughout the specified time frame of (2009–2023). The NDBI showed an increasing trend in the LST suggesting significant urbanization occurring outside the research region. (Fig. 9a-c) illustrates a regression study including the five variables mentioned: LST, NDVI, NDWI, month, and NDBI. Conversely, the study area exhibited a lower level of urbanization. According to (Rahman et al. 2020), the NDWI result indicated a decrease in air humidity and hydraulic stress in 2012 (Byomkesh et al. 2012; Dewan et al. 2012). In contrast, the NDBI value exhibited a progressive increase, which corresponded to greater LST values (Fig. 9a-c). The regression analysis and multiple correlation analyses reveal that LST has a robust and positive association with NDBI, whereas it demonstrates a substantial, low-impact relationship with NDVI, NDWI, and NDBI (Fig. 9a-c). LST indices, with R^2 values of (0.42–0.68) for NDVI and NDWI (negative correlation) and (0.04–0.26) for NDBI (positive correlation). The R^2 values ranging from 0.42 to 0.68 for NDVI and NDWI, which exhibit a negative correlation, indicate a reduction in vegetation and water bodies and the same evaluation has been shown in (Kafy et al. 2020). Conversely, the NDBI value ranges from 0.04 to 0.26, indicating a positive connection that shows an increase in built areas owing to heightened urbanization in DMDP regions. Economic factors such as land subsidies, price escalations, and taxation influence human decision-making and land utilization (Kafy et al. 2020).

Table 4 demonstrates the correlation coefficient, which indicates the degree of influence one component has on another variable. To dive more into the correlation of indices, in 2009, the correlation between LST and NDBI is weak (R^2 =0.04733) (Table 4), suggesting minimal linear association between urban built-up areas and surface temperature during this period. The correlation between LST and NDVI suggests a moderate positive correlation (R^2 = 0.42608). This indicates a stronger relationship between vegetation and LST, where increasing vegetation likely influences surface temperature patterns to some extent.

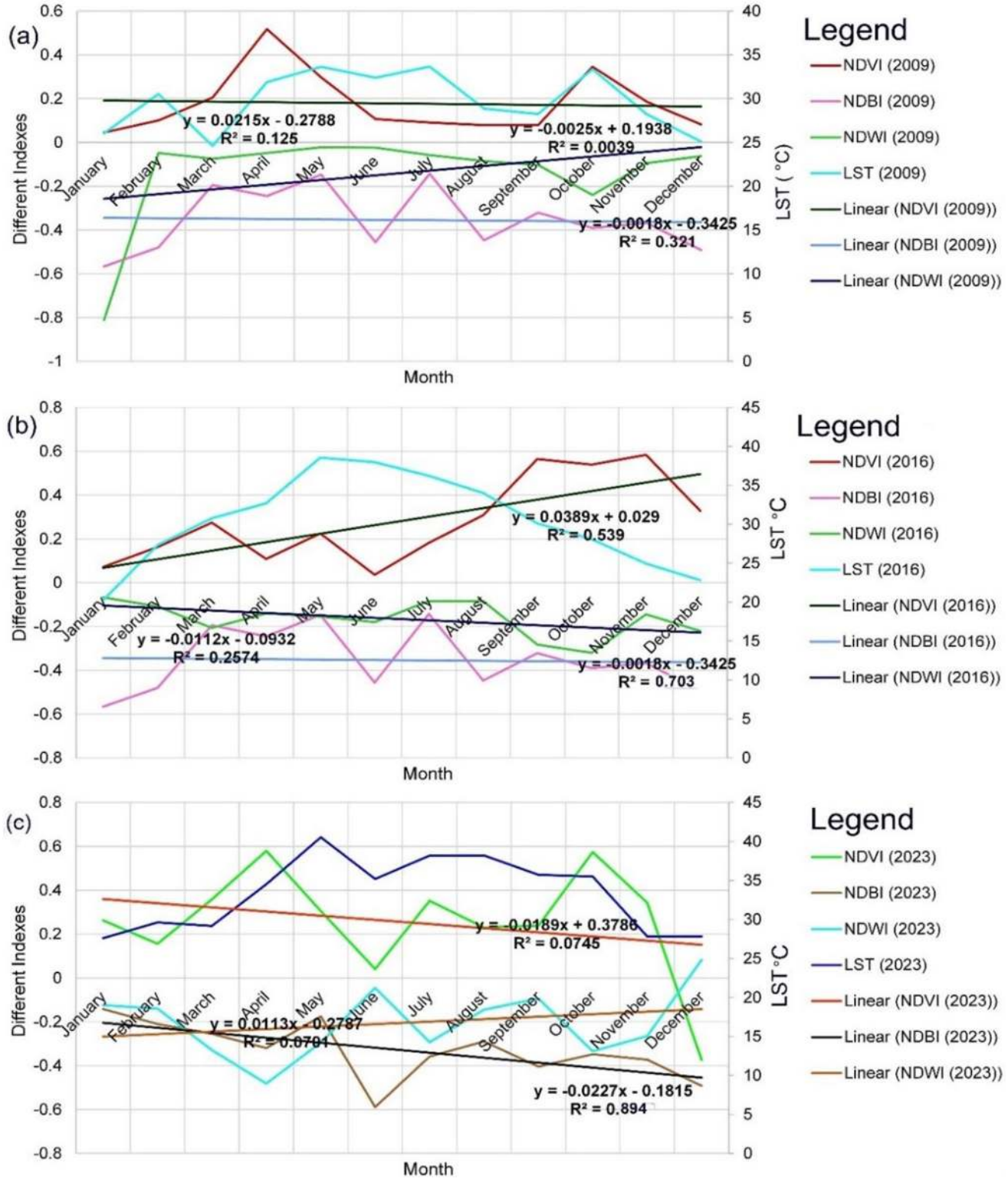

Fig. 9 Liner regression analysis of LST and indexes (**a**) 2009, (**b**) 2016 & (**c**) 2023

Table 4 The coefficient of correlation between LST and NDVI, NDVI, NDBI in the research area

2009	LST	NDBI	NDVI	NDWI
LST	1			
NDBI	0.04733	1		
NDVI	0.42608	0.03933	1	
NDWI	0.32443	-0.09873	0.23329	1
2016	**LST**	**NDBI**	**NDVI**	**NDWI**
LST	1			
NDBI	0.52373	1		
NDVI	0.23431	-0.18676	1	
NDWI	-0.68707	0.1159	-0.81981	1
2023	**LST**	**NDBI**	**NDVI**	**NDWI**
LST	1			
NDBI	0.62234	1		
NDVI	0.06063	0.01234	1	
NDWI	-0.0892	-0.23604	-0.8955	1

LST also shows a moderate positive correlation with NDWI ($R^2 = 0.32443$). This suggests that water bodies have some influence on LST, possibly reflecting cooling effects from water presence (Figs. 4 and 8). This overall correlation with LST in the year 2009 indicates that the presence of the water bodies, and green areas in the research region is growing due to the abundance of built-up areas. In 2016, the correlation between LST and NDBI strengthens significantly compared to 2009, indicating a stronger association between built-up areas and rising surface temperatures as $R^2 = 0.52373$. This could lead to increased urbanization and its heat island effect. Consequently, the relationship between LST and NDVI weakens ($R^2 = 0.23431$) compared to 2009, suggesting that the impact of vegetation on surface temperature may have lessened or become more complex during this period. The correlation between LST and NDWI ($R^2 = -0.68707$) becomes strongly negative. This means that as the presence of water bodies increases, surface temperatures tend to decrease, indicating a cooling effect of water in this period possibly due to heavy rainfall and more greening of the adjacent vegetations as seen on the northeastern part of the study area. In 2023, the positive correlation between LST and NDBI ($R^2 = 0.62234$) continues to strengthen, showing a strong association between urban built-up areas and increasing surface temperatures, likely due to further urbanization. On the other hand, correlation between LST and NDVI ($R^2 = 0.06063$) drops to near zero, indicating a very weak relationship between vegetation and surface temperature in 2023. The negative correlation between LST and NDWI ($R^2 = -0.68707$) becomes weaker compared to 2016. While water still has a cooling effect on surface temperatures, the relationship is much less pronounced than in the earlier period. Temperature has increased in the northwestern part of the study area while decreased in the upper regions (Figs. 4, 8 and 10). While the major structural construction has started in the lower (southeast) region of DMDP area, and the upper (northeastern) region has already lost vegetation in earlier years; the correlation reflects the probable connection of changing pattern of LST in these two regions. Overall, the land use and land cover played a significant role in these changing patterns of temperature in DMDP. LST rises with growth in urbanised and barren terrain, whereas it diminishes with the expansion of forests, agricultural land, wetlands, and water regions (A.-A. Kafy et al. 2021; A.-A. Kafy, M. N. H. Naim, et al., 2021). According to the findings, there has been a significant decrease in green areas and a corresponding increase in built-up regions, resulting in a substantial shift in surface temperature. The rapid transition from vegetation and waterbody regions to built-up and urban areas is significantly impacting the (LST) in a more vulnerable manner this year. This unfavorable connection was the greatest seen throughout the research period. Because of the intricate nature of landscape conditions, the LST-NDBI constructs robust relationships, and it indicates that the LST-NDVI and LST-NDWI tend to have somewhat weaker correlations.

4.6 Relationship between LULC and LST

The outermost layer of the Earth comprises various land coverings, including structures, manufacturing regions, roadways, forests, exposed soil, and waterways (such as rivers, canals, and ponds) (Dewan et al. 2012). The electromagnetic radiation emitted by these interface elements can be detected and measured using remote sensing technology, namely via the use of land surface temperature LST measurements (A.-A. Kafy et al. 2021; Kafy et al. 2020). The entire study area demonstrated LULC and LST, as shown in (Figs. 4 and 10), which depict the median LST for each type of LULC. The central portion of the study region in 2009 experienced a greater concentration of LST values due to the presence of the main metropolitan area. On the contrary, the urban area (149.563 km^2) has increased, whereas the total area of vegetation (69.563 km^2) and waterbodies (80.3461 km^2) have decreased (Table 3). During these periods (2009–2023), there was a decrease in greenery in the northeastern region, which was higher after 2016 while the urban area expanded. This had a significant impact on the whole city temperature, and the north-east area shows the high effect of LST. Figure 9(a-c) demonstrates that the NDBI has grown in the main metropolitan area, which comprises most of the developed areas. In 2009, the average peak LST was around 34 °C, which rose to above 36 °C in 2016 and over 38 °C in 2023. The rise in NDBI corresponded to an increase in temperature after 2016, whereas vegetation and water areas had a decline during this time.

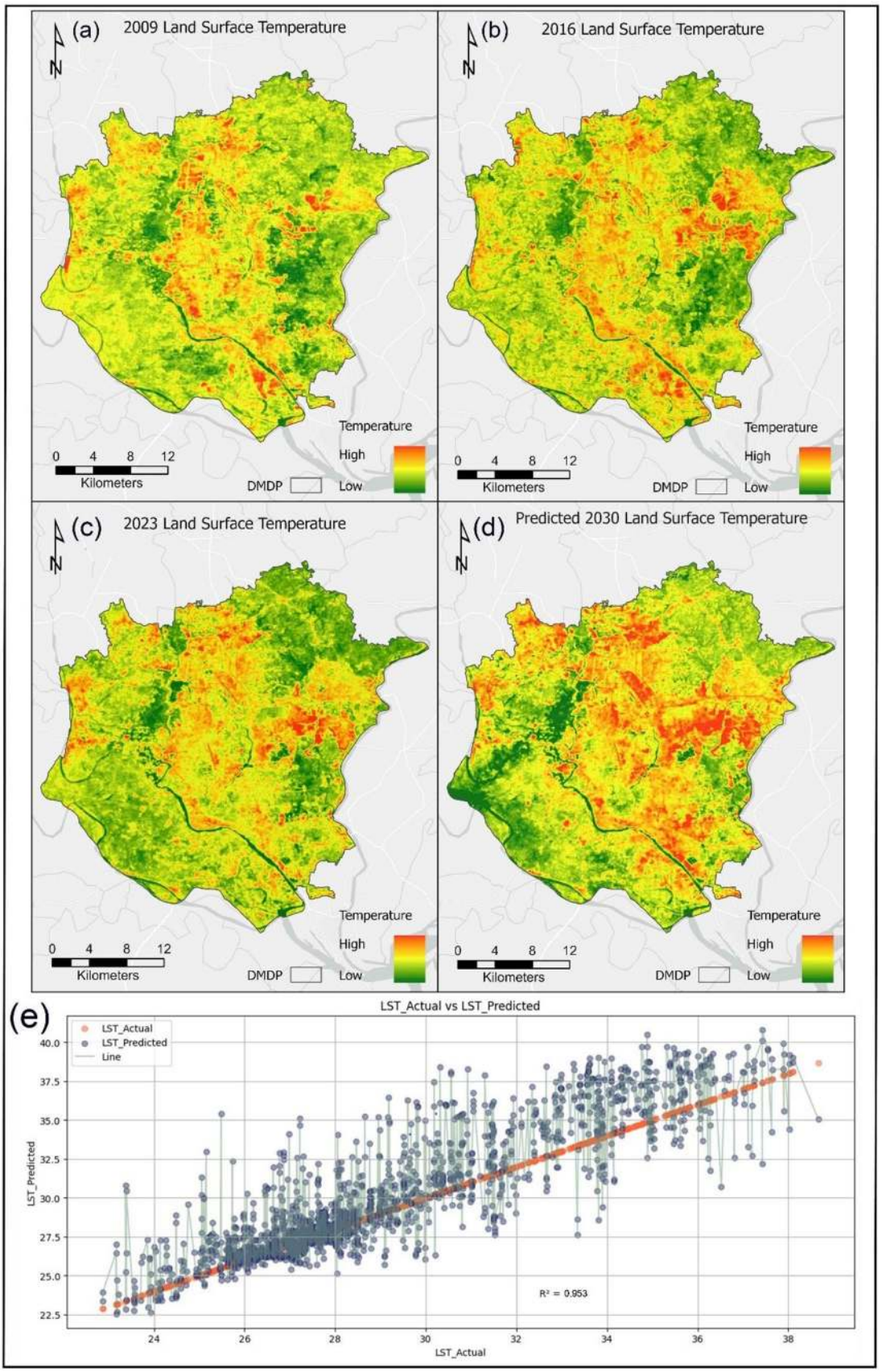

Fig. 10 LST observation in the study area: (**a**) 2009, (**b**) 2016, (**c**) 2023, (**d**) Predicted LST for 2030, and (**e**) Actual vs Precited LST

4.7 LST prediction for 2030

The LULC scenarios, the research period from 2009 to 2023 shows a noticeable change in the study area's LST. Hence, the LST was simulated for three different periods 2009, 2016 and 2023 (Fig. 10a-c). The random foresthistorically estimated LST data patterns to forecast future LST trends in the study area (Fig. 10a-c). Since the simulation was based on previous LST regression analysis (Fig. 10e) trends from to 2023, the prevalence of higher LST in urban areas had an impact on the simulation. The effect of greenhouse gases on global warming and changes in surface features are other factors that may contribute to an increase in LST, even in the absence of rapid urbanization. The scatterplots in (Fig. 10e) demonstrate the comparison between the observed LST and the predicted LST applying the LST framework. The regression coefficient of determination (R^2) for the model-predicted vs actual values is 0. 0.953, which is greater than the R^2 scores of the LULC indexes vs LST (Fig. 10e). The abbreviation (Fig. 10e) denotes that there exists a robust correlation among the actual and projected values in the model. Based on this investigation, it is evident that the LST model produced LST values that were very near to the real values. Figure 10e displays the scatterplots that compare the observed LST with the predicted LST obtained from the LST model. The coefficient of determination (R^2) reaches the high range on prediction 0.61 (Fig. 10e), indicating a robust correlation between the actual and model-predicted variables. Based on this investigation, it is evident that the LTS model produced LST values near the actual values. Therefore, the model is suitable for making highly accurate predictions of LST. Hence, the model utilizes LST impacts. Based on the provided graphs and scatter plots, it can be inferred that the model can accurately forecast LST values. Therefore, it can be inferred that the model is suitable for making very accurate predictions of LST, as seen in (Fig. 10d). The LST was lower, as shown by (Fig. 10a), in places where urban development in the north-south direction was similarly low, as shown in Fig. 7a. However, the urban growth in these areas rose between 2015 and 2016 due to the DMDP project and it directly effects the ecosystems. Ecosystems are complex spatial-temporal human-environment interactions. Temporal elements are as crucial as spatial ones in landscape change in this research, which impact LST beyond the physical LULC changes (Figs. 4 and 10). Ecological and socioeconomic factors influence these changes. Multiple socioeconomic concerns were analyzed by including data on demographics, employment, economics, infrastructure's economic structure, and government (Islam et al. 2015). The relationships between intervals of land-cover data and socioeconomic indicators were analyzed using redundancy analysis. The correlation coefficients have been applied to ascertain critical socio-economic variables of land-cover alterations(Ismail and Jusoff 2008). The findings indicated that a significant proportion of variation in land-cover data may be attributed to socio-economic variables. Land-cover change types may be described by combinations of essential socio-economic factors. The indicators may assist in reconstructing land-cover changes in different locations. Consequently, they provide a foundation for the establishment of ecologically sound land-cover management processes. This rise in urban growth had an impact on the total temperature of the city, as seen in Fig. 10b.According to (Fig. 10c), where LULC change was higher, and it indicated that (Fig. 8) vegetation and water-body are also lower. On the other hand, urban and build up area has also increased in 2030 with temperature rise is upto 41 °C which is higher than last several years. Based on the provided graphs and scatter diagrams, it can be inferred that the model has the ability to accurately forecast LST values.

The predictive results demonstrate that LST has risen in the past few decades (2009–2023), with urbanised regions contributing to the prevalence of elevated LST. The expansion of metropolitan areas and a significant reduction in plant cover would substantially elevate land surface temperatures, hence exacerbating urban heat island effects. In the absence of urbanization, potential factors contributing to the increase in temperature include changes in greenhouse effects, climate change, and surface features. The projected land surface temperature revealed the actual dangers associated with the ongoing temperature increase, including intensified urban heat island impacts. Power consumption, elevated emissions of greenhouse gases, and air pollution together exacerbate the UHI impact, endangering aquatic ecosystems (rivers, lakes, ponds, streams, and seas) and presenting risks to human health. Elevated greenhouse gas emissions predominantly detriment human health, diminish urban health quality and compromise the environmental sustainability of cities.

5 Limitations

The SVM has been used in this research for LULC analysis and it robust the adaptable machine learning technique, but with constraints like computational cost, hyperparameter optimization, and uneven class distributions. Notwithstanding these factors, it provides precise classification and prediction answers across several domains, establishing it as a fundamental approach in machine learning. In here for LST analysis, RF with an ensemble method, provides precise forecasts; nevertheless, its intricate decision-making process, processing demands, and hyperparameter optimization might diminish interpretability. It may encounter difficulties with skewed datasets. Even cloud covering was a major issue for

these kinds of studies (Tadese et al. 2020; Yin et al. 2010) but in here it was tried to be declined (~ 2%). The overall system does not have any criteria that have been set for the individual weighting of each parameter that is supplied as input (Kafy et al. 2020). However, it is not feasible to make predictions with a 100% reliability about changing events like as urbanization, the loss of green cover, and the increasing number of surface temperatures. This is due to the fact that these phenomena are primarily influenced by the activities of humans and rational choices made at the regional to metropolitan level.

6 Conclusion

This study utilized Landsat satellite images to observe and reflect the alterations in LULC in DMDP, Bangladesh. The study demonstrated that there has been an extensive change in LULC in the DMDP area from 2009 to 2023. The most notable changes occurred in the conversion of vegetation and waterbody areas. During this time frame, the vegetation area decreased by 16.7081% (61.3461km^2) and the waterbody area decreased by 51.713% (80.3461km^2). Conversely, settlements in cities witnessed a significant rise of 67.81% (149.563km^2). The growth of urban regions was particularly intense in the north, south, and east directions. LST also has a strong co-relationship with NDBI where there is a lower correlation, and it revealed that build-up area is increasing on the other hand vegetation and waterbody are decreasing. That resulted in the LST value increasing where the average value was (37 °C to 39 °C) and the predicted value has been increased to 41 °C. This rapid urban expansion, achieved by transforming the earth's resources, has significant environmental impacts, including the reduction of ecological services, and a decline in land available for agricultural output, the rise in extreme temperatures, and the emergence of associated with illness. The growth of urban areas is resulting of ecological consequences, including the depletion of biodiversity, the intensification of heat waves, and the emergence of health problems. To address these problems, it is necessary to implement adaptive land management plans that use satellite imagery detail planning DMDP. This research aims to assist the authorities, policy makers, lawmakers, and city planners in using the microlevel directional strategy in DMDP. This DMDP dynamic modeling indicates how can reduce urban heat island effects by incorporating LULC modeling, promoting greening, and implementing sustainable urban layouts, thereby creating a cooler, pedestrian-friendly environment. The goal is to create livable cities, preserve water bodies, and plan urban construction in a way that is equitable and ecologically responsible for DMDP.

Future research may examine the possibility of including other spectral measurements, such as the Soil Adjusted Vegetation Index (SAVI) or the Enhanced Vegetation Index (EVI), by establishing a correlation between LST and these different indices. There is a possibility that it will provide an improved relationship with the LST in some regions. In addition, the use of indices that place a focus on anthropogenic causes, such as the Oblivious Surface Area Index (ISA), may give a more comprehensive understanding of the human impacts that are exerted on LST with urbanization.

Supplementary Information The online version contains supplementary material available at https://doi.org/10.1007/s00704-024-05264-3.

Acknowledgements Not applicable.

Author contributions **M Shahriar Sonet**: Writing – review & editing, Writing – original draft, Visualization, Validation, Supervision, Software, Resources, Project administration, Methodology, Investigation, Formal analysis, Data curation, Conceptualization. **Md Yeasir Hasan**: Writing – review & editing, Writing – original draft, Visualization, Validation, Supervision, Methodology, Formal analysis, Data curation. **Abdulla Al Kafy**: Writing – review & editing, Supervision, Resources, Project administration, Methodology, Investigation, Data curation. **Nobonita Shobnom**: Writing – review & editing, Writing – original draft, Validation, Supervision, Resources, Methodology, Investigation, Formal analysis.

Funding No funding was received.

Data availability No datasets were generated or analysed during the current study.

Declarations

Ethical approval Not applicable.

Consent to participate Not applicable.

Consent for publication Not applicable.

Competing interests The authors declare no competing interests.

References

Abdullah AYM, Masrur A, Adnan MSG, Baky MAA, Hassan QK, Dewan A (2019) Spatio-temporal patterns of land use/land cover change in the heterogeneous coastal region of Bangladesh between 1990 and 2017. Remote Sens 11(7):790. https://doi.org/10.3390/rs11070790

Ahmed B (2011) Urban land cover change detection analysis and modeling spatio-temporal growth dynamics using Remote sensing and GIS techniques: a case study of Dhaka, Bangladesh. Universidade NOVA de Lisboa (Portugal)

Ahmed MT, Hasan MY, Khan AS, Hasan M (2019) Valuation of Irrigation Water at Shagordari, Jashore, Bangladesh. Int Res J Eng Technol (IRJET) 06(11):1050–1057

Ahmed MT, Hasan MY, Monir MU, Samad MA, Rahman MM, Rifat I, Jamil MS, M. N (2020a) Evaluation ofhydrochemical properties and groundwater suitability for irrigation uses in southwestern

zones of Jashore, Bangladesh. Groundw Sustainable Dev 11:100441. https://doi.org/10.1016/j.gsd.2020.100441

Ahmed MT, Islam MN, Hasan MY, Uddin M, Monir ASK, Rahman MM (2020b) Monitoring of GroundwaterQuality in Arsenic and Salinity Prone areas of Jashore, Bangladesh. Int J Econ Environ Geol 11(1):83–88. https://doi.org/10.46660/ijeeg.Vol11.Iss1.2020.417

Ahmed MT, Monir MU, Hasan MY, Rahman MM, Rifat MSI, Islam MN, Islam MS (2020c) Hydro-geochemical evaluation of groundwater with studies on water quality index and suitability for drinking in Sagardari, Jashore. J Groundw Sci Eng 8(3):259–273. https://doi.org/10.19637/j.cnki.2305-7068.2020.03.006

Ahmed MT, Monir MU, Aziz AA, Hasan Y, Khan MFH, Islam K, Samad A (2022) Hydrochemical investigations of coastal aquifers and saltwater intrusion in severely affected areas of Satkhira and Bagerhat districts, Bangladesh. Arab J Geosci 15(8):1–22. https://doi.org/10.1007/s12517-022-09955-x

Aldino AA, Saputra A, Nurkholis A, Setiawansyah S (2021) Application of support Vector Machine (SVM) Algorithm in classification of Low-Cape communities in Lampung Timur. Building Inf Technol Sci (BITS) 3(3):325–330. https://doi.org/10.47065/bits.v3i3.1041

Avdan U, Jovanovska G (2016) Algorithm for automated mapping of land surface temperature using LANDSAT 8 satellite data. J Sens 2016:1–8. https://doi.org/10.1155/2016/1480307

Background MI Normalized Difference Built-Up Index (NDBI). *Harris Geospatial Solutions. URL: Available from: http://www.harrisgeospatial.com/docs/BackgroundOtherIndices. html [Accessed: 27 January 2016]*

BBS S (1998) Statistical year book of Bangladesh. *Bangladesh Bureau of Statistics Division, Ministry of Planning, Government of the People Republic of Bangladesh, Dhaka, Bangladesh*

BMD B (2013) Country report: Bangladesh meteorological department (BMD)

Byomkesh T, Nakagoshi N, Dewan AM (2012) Urbanization and green space dynamics in Greater Dhaka, Bangladesh. Landscape Ecol Eng 8:45–58. https://doi.org/10.1007/s11355-010-0147-7

Cao H, Liu J, Chen J, Gao J, Wang G, Zhang W (2019) Spatiotemporal patterns of urban land use change in typical cities in the Greater Mekong Subregion (GMS). Remote Sens 11(7):801. https://doi.org/10.3390/rs11070801

Climate E (2020) Dhaka Climate (Bangladesh)[WWW Document]. https://enclimate-dataorg/asia/bangladesh/dhaka-division/dhaka-1062098.

Dai L, Wörner R, van Rijswick HF (2018) Rainproof cities in the Netherlands: approaches in Dutch water governance to climate-adaptive urban planning. Int J Water Resour Dev 34(4):652–674. https://doi.org/10.2166/ws.2014.127

Dewan AM, Kabir MH, Nahar K, Rahman MZ (2012) Urbanisation and environmental degradation in Dhaka Metropolitan Area of Bangladesh. Int J Environ Sustain Dev 11(2):118–147. https://doi.org/10.1504/IJESD.2012.049178

Ahmed MT, Hasan MY, Monir MU, Biswas BK, Quamruzzaman C, Junaid M, Rahman MM (2021) Evaluationof groundwater quality and its suitability by applying the geospatial and IWQI techniques for irrigationpurposes in the southwestern coastal plain of Bangladesh. Arab J Geosci 14(3):1–24. https://doi.org/10.1007/s12517-021-06510-y

Faruque MJ, Vekerdy Z, Hasan MY, Islam KZ, Young B, Ahmed MT, Kundu P (2022) Monitoring of land use and land cover changes by using remote sensing and GIS techniques at human-induced mangrove forests areas in Bangladesh. Remote Sens Applications: Soc Environ 25:100699. https://doi.org/10.1016/j.rsase.2022.100699

Han H, Yang C, Song J (2015) Scenario simulation and the prediction of land use and land cover change in Beijing, China. Sustainability 7(4):4260–4279. https://doi.org/10.3390/su7044260

Hassan MM, Southworth J (2017) Analyzing land cover change and urban growth trajectories of the mega-urban region of Dhaka using remotely sensed data and an ensemble classifier. Sustainability 10(1):10. https://doi.org/10.3390/su10010010

Hoque M, Phinn S, Roelfsema C, Childs I (2016a) *Modelling tropical cyclone hazards under climate change scenario using geospatial techniques.* Paper presented at the IOP conference Series: Earth and environmental science

Hoque MAA, Phinn S, Roelfsema C, Childs I (2016b) Assessing Tropical Cyclone impacts using object-based moderate spatial resolution image analysis: a Case Study in Bangladesh. Int J Remote Sens 37(22):5320–5343. https://doi.org/10.1080/01431161.2016.1239286

Hossain MS, Rahman M (2022) *Assessment of Land Use/Land Cover (LULC) Changes and Urban Growth Dynamics Using Remote Sensing in Dhaka City, Bangladesh.* Paper presented at the ICSBE 2020: Proceedings of the 11th International Conference on Sustainable Built Environment

Islam MS, Uddin MK, Tareq SM, Shammi M, Kamal AKI, Sugano T, Kuramitz H (2015) Alteration of water pollution level with the seasonal changes in mean daily discharge in three main rivers around Dhaka City, Bangladesh. Environments 2(3):280–294. https://doi.org/10.3390/environments2030280

Islam MA, Paull DJ, Griffin AL, Murshed S (2020) Assessing ecosystem resilience to a tropical cyclone based on ecosystem service supply proficiency using geospatial techniques and social responses in coastal Bangladesh. Int J Disaster Risk Reduct 49:101667. https://doi.org/10.1016/j.ijdrr.2020.101667

Ismail MH, Jusoff K (2008) Satellite data classification accuracy assessment based from reference dataset. Int J Geol Environ Eng 2(3):23–29

Justice C, Giglio L, Korontzi S, Owens J, Morisette J, Roy D, Kaufman Y (2002) The MODIS fire products. Remote Sens Environ 83(1–2):244–262. https://doi.org/10.1016/S0034-4257(02)00076-7

Kafy AA, Faisal A-A, Sikdar S, Hasan M, Rahman M, Khan MH, Islam R (2020) Impact of LULC changes on LST in Rajshahi district of Bangladesh: a remote sensing approach. J Geographical Stud 3(1):11–23. https://doi.org/10.1016/j.rsase.2022.100886

Kafy A-A, Al Rakib A, Akter KS, Jahir DMA, Sikdar MS, Ashrafi TJ, Rahman MM (2021) Assessing and predicting land use/land cover, land surface temperature and urban thermal field variance index using landsat imagery for Dhaka Metropolitan area. Environ Challenges 4:100192. https://doi.org/10.1016/j.envc.2021.100192

Kafy A-A, Al Rakib A, Roy S, Ferdousi J, Raikwar V, Kona MA, Al Fatin SA (2021b) Predicting changes in land use/land cover and seasonal land surface temperature using multi-temporal landsat images in the northwest region of Bangladesh. Heliyon 7(7). https://doi.org/10.1016/j.heliyon.2021.e07623

Kafy A-A, Islam M, Sikdar S, Ashrafi TJ, Al-Faisal A, Islam MA, Ali MY (2021c) Remote sensing-based approach to identify the influence of land use/land cover change on the urban thermal environment: a case study in Chattogram City, Bangladesh. Re-envisioning remote sensing applications. CRC, pp 217–240

Kafy A-A, Naim MNH, Subramanyam G, Ahmed NU, Rakib A, Kona A, M. A., Sattar GS (2021d) Cellular Automata approach in dynamic modelling of land cover changes using RapidEye images in Dhaka, Bangladesh. Environ Challenges 4:100084. https://doi.org/10.1016/j.envc.2021.100084

Kafy AA, Faisal A-A, Al Rakib A, Roy S, Ferdousi J, Raikwar V, Fatin SMAA (2021e) Predicting changes in land use/land cover and seasonal land surface temperature using multi-temporal landsat images in the northwest region of Bangladesh. Heliyon 7(7):e07623. https://doi.org/10.1016/j.heliyon.2021.e07623

Karim MF, Mimura N (2008) Impacts of Climate Change and Sea-Level rise on Cyclonic Storm Surge floods in Bangladesh. Glob

Environ Change 18(3):490–500. https://doi.org/10.1016/j.gloenvcha.2008.05.002
Khan M (2014) Study of open spaces in the context of Dhaka city for sustainable use: a syntactic approach. Int J Eng Technol 6(3):238–243. https://doi.org/10.7763/IJET.2014.V6.704
Khan MMH, Bryceson I, Kolivras KN, Faruque F, Rahman MM, Haque U (2015) Natural disasters and land-use/land-cover change in the southwest coastal areas of Bangladesh. Reg Envriron Chang 15:241–250. https://doi.org/10.1007/s10113-014-0642-8
Li H, Xiao P, Feng X, Yang Y, Wang L, Zhang W, Chang X (2017a) Using land long-term data records to map land cover changes in China over 1981–2010. IEEE J Sel Top Appl Earth Observations Remote Sens 10(4):1372–1389. https://doi.org/10.1109/JSTARS.2016.2645203
Li Y, Cao Z, Long H, Liu Y, Li W (2017b) Dynamic analysis of ecological environment combined with land cover and NDVI changes and implications for sustainable urban–rural development: the case of Mu us Sandy Land, China. J Clean Prod 142:697–715. https://doi.org/10.1016/j.jclepro.2016.09.011
Liu C, Frazier P, Kumar L (2007) Comparative assessment of the measures of thematic classification accuracy. Remote Sens Environ 107(4):606–616. https://doi.org/10.1016/j.rse.2006.10.010
Mallick B, Ahmed B, Vogt J (2017) Living with the risks of cyclone disasters in the southwestern coastal region of Bangladesh. Environments 4(1):13
Mansaray AS, Dzialowski AR, Martin ME, Wagner KL, Gholizadeh H, Stoodley SH (2021) Comparing PlanetScope to Landsat-8 and Sentinel-2 for sensing water quality in reservoirs in agricultural watersheds. Remote Sens 13(9):1847. https://doi.org/10.3390/rs13091847
Morshed N, Yorke C, Zhang Q (2017) Urban expansion pattern and land use dynamics in Dhaka, 1989–2014. Prof Geogr 69(3):396–411. https://doi.org/10.1080/00330124.2016.1268058
Naserikia M, Asadi Shamsabadi E, Rafieian M, Leal Filho W (2019) The Urban Heat Island in an urban context: a case study of Mashhad, Iran. Int J Environ Res Public Health 16(3):313. https://doi.org/10.3390/ijerph16030313
Olofsson P, Foody GM, Herold M, Stehman SV, Woodcock CE, Wulder MA (2014) Good practices for estimating area and assessing accuracy of land change. Remote Sens Environ 148:42–57. https://doi.org/10.1016/j.rse.2014.02.015
Rabe A, van der Linden S, Hostert P (2010) *Simplifying Support Vector Machines for classification of hyperspectral imagery and selection of relevant features.* Paper presented at the 2010 2nd Workshop on Hyperspectral Image and Signal Processing: Evolution in Remote Sensing
Rahman MM, Avtar R, Yunus AP, Dou J, Misra P, Takeuchi W, Kurniawan TA (2020) Monitoring effect of spatial growth on land surface temperature in Dhaka. Remote Sens 12(7). https://doi.org/10.3390/rs12071191
Rahman MM, Haque T, Mahmud A, Al Amin M, Hossain MS, Hasan MY, Bai L (2023) Drinking water quality assessment based on index values incorporating WHO guidelines and Bangladesh standards. Phys Chem Earth Parts A/B/C 129:103353. https://doi.org/10.1016/j.pce.2022.103353
Reis S (2008) Analyzing land use/land cover changes using remote sensing and GIS in Rize, North-East Turkey. Sensors 8(10):6188–6202. https://doi.org/10.3390/s8106188
Rouse JW, Haas RH, Schell JA, Deering DW (1974) Monitoring vegetation systems in the Great Plains with ERTS. NASA Spec Publ 351(1):309
Roy B, Bari E (2022) Examining the relationship between land surface temperature and landscape features using spectral indices with Google Earth Engine. Heliyon 8(9). https://doi.org/10.1016/j.heliyon.2022.e10668
Roy B, Bari E, Nipa NJ, Ani SA (2021) Comparison of temporal changes in urban settlements and land surface temperature in Rangpur and Gazipur Sadar, Bangladesh after the establishment of city corporation. Remote Sens Applications: Soc Environ 23:100587. https://doi.org/10.1016/j.rsase.2021.100587
Siddiqua F (2017) Dhaka needs more trees, but…. Dly Star. https://www.thedailystar.net/star-weekend/dhaka-needs-more-trees-1414189
Simon O, Lyimo J, Yamungu N (2024) Exploring the impact of socioeconomic factors on land use and cover changes in Dar Es Salaam, Tanzania: a remote sensing and GIS approach. Arab J Geosci 17(3):99. https://doi.org/10.1007/s12517-024-11908-5
Sonet MS, Hasan MY, Chakma S, Al Kafy A (2024) Assessing tropical cyclone impacts in coastal Bangladesh: a change detection analysis on cyclone bulbul using geospatial analysis and remote sensing techniques. Int J Disaster Risk Reduct 112:104726. https://doi.org/10.1016/j.ijdrr.2024.104726
Tadese M, Kumar L, Koech R, Kogo BK (2020) Mapping of land-use/land-cover changes and its dynamics in Awash River Basin using remote sensing and GIS. Remote Sens Applications: Soc Environ 19:100352. https://doi.org/10.1016/j.rsase.2020.100352
Ullah S, Ahmad K, Sajjad RU, Abbasi AM, Nazeer A, Tahir AA (2019) Analysis and simulation of land cover changes and their impacts on land surface temperature in a lower himalayan region. J Environ Manage 245:348–357. https://doi.org/10.1016/j.jenvman.2019.05.063
Ullah M, Li J, Wadood B (2020) Analysis of urban expansion and its impacts on land surface temperature and vegetation using RS and GIS, a case study in Xi'an City, China. Earth Syst Environ 4(3):583–597
Wang F, Xu YJ (2010) Comparison of remote sensing change detection techniques for assessing hurricane damage to forests. Environ Monit Assess 162(1):311–326
Ward PJ, Marfai MA, Yulianto F, Hizbaron D, Aerts J (2011) Coastal inundation and damage exposure estimation: a case study for Jakarta. Nat Hazards 56:899–916. https://doi.org/10.1007/s11069-010-9599-1
Xu H (2006) Modification of normalised difference water index (NDWI) to enhance open water features in remotely sensed imagery. Int J Remote Sens 27(14):3025–3033. https://doi.org/10.1080/01431160600589179
Xu X, Shrestha S, Gilani H, Gumma MK, Siddiqui BN, Jain AK (2020) Dynamics and drivers of land use and land cover changes in Bangladesh. Reg Envriron Chang 20(2):54. https://doi.org/10.1007/s10113-020-01650-5
Yin J, Xu S, Wang J, Zhong H, Hu Y, Yin Z, Zhang X (2010) Vulnerability assessment of combined impacts of sea level rise and coastal flooding for China's coastal region using remote sensing and GIS. *18th International Conference on. IEEE*, 1–4
Yirsaw E, Wu W, Shi X, Temesgen H, Bekele B (2017) Land use/land cover change modeling and the prediction of subsequent changes in ecosystem service values in a coastal area of China, the Su-Xi-Chang Region. Sustainability 9(7):1204. https://doi.org/10.3390/su9071204
Zha Y, Gao J, Ni S (2003) Use of normalized difference built-up index in automatically mapping urban areas from TM imagery. Int J Remote Sens 24(3):583–594. https://doi.org/10.1080/01431160304987
Zhang XY, Wang Y, Jiang H, Wang XM (2013) Remote-sensing Assessment of Forest damage by Typhoon Saomai and its related factors at Landscape Scale. Int J Remote Sens 34(21):7874–7886. https://doi.org/10.1080/01431161.2013.827344